2012

The effect of tow grouping resolution on shearing deformation of unidirectional non-crimp fabric

Wade Johanns
Iowa State University

The effect of tow grouping resolution on shearing deformation of unidirectional non-crimp fabric

by

Wade Walter Johanns

A thesis submitted to the graduate faculty
in partial fulfillment of the requirements for the degree of
MASTER OF SCIENCE

Major: Industrial Engineering

Program of Study Committee:
John Jackman, Major Professor
Vinay Dayal
Matthew Frank
Frank Peters

Iowa State University
Ames, Iowa
2012

Table of Contents

List of Figures

List of Tables

Acknowledgements

I would like to thank my major professor, Dr. John Jackman, for all of his support and masterful editing assistance, my committee members Dr. Matt Frank, Dr. Frank Peters, and Dr. Vinay Dayal for bringing me on to the AMII project in record time and providing me with great resources and guidance, and Steve Nolet for his encouragement.

I would like to thank Kevin Brownfield for building anything I asked him with little instruction including the shearing device that made this project possible, Camila Dantas, my wonderful URA, for producing and measuring all of the samples, and all of the WEML students.

Team PrISUm deserves some thanks for moving so that I could keep the same office and desk in 'Old' Sweeney and for providing some relief from my work.

I especially would like to thank my family for all of their support during my long duration at Iowa State and Erin Kelly for always being there for me and keeping me on track when things were difficult and I needed it most.

Abstract

In the rapidly growing large-scale composites industry, specifically in the area of wind turbine blade manufacturing, reducing costs through reduced man-hours and materials while simultaneously increasing quality has become a major focus. One strategy is to automate the manual lay-up process. Automation techniques used in the aerospace industry are too costly for wind turbine blade manufacturing; therefore, new techniques need to be investigated. This research describes a new fabric pre-shearing process to reduce out-of-plane deformations during the lay-up process that enables automated deposition of unidirectional non-crimp fabrics (NCF) in molds. This new process controls the manipulation of broad-loom NCF fabrics such that fabric geometry is well controlled, reducing the need for naïve and inconsistent manual lay-ups.

Previous research modeled the behavior of NCF fabric in order to predict the final characteristics of the fabric after shearing. However, this model was never validated with NCF fabric. The goal of this research was to determine the effects of shearing process parameters on NCF fabric geometry and validate the predicted characteristics generated by the previous shearing model. An empirical study of fabric shearing was conducted and the analysis of fabric samples transformed by the pre-shearing process is presented. A comparison of the conformance of un-sheared fabrics to pre-sheared fabrics shows that fabric pre-shearing reduces out-of-plane deformations and produces consistent fabric geometry.

Chapter 1. Introduction

Background

Composite materials are increasingly being used in a wide variety of new products that require low weight and high strength. The term composite indicates that the material is made from two different types of material, namely, a reinforcement component and a binding matrix. Typical reinforcement components are fibers such as glass, carbon, or polymer which are then infused with a binding matrix such as a polymer resin. The fiber components exhibit high tensile yields when loaded in the direction of the fibers and when combined with the polymer resin achieve a high stiffness. Composites also exhibit high fatigue lives, which is useful for cyclically loaded parts. These materials can be found in products ranging from snowboards to large aircraft.

With the increased usage of composites, the relationship between product geometry and fiber geometry has become more important because this relationship affects the mechanical properties of the final product. Reinforcing fibers create the strongest and stiffest parts when they are allowed to be as long as possible with only small angular deviations from a linear path. There are multiple methods for producing composite parts including open-mold wet lay-up, closed-mold wet lay-up, pultrusion, vacuum assisted resin transfer molding (VARTM), light resin transfer molding (LRTM), autoclaving of pre-pregs, and filament winding (Gutowski 1997). Each method uses a different combination of fiber placement and resin application. The most common form of reinforcing fibers is a thin fabric sheet or ply. This is due to the anisotropic mechanical properties of the fibers. The fibers exhibit the highest strength when loaded along their length and a have a high strength to weight ratio compared to structural metal alloys. The plies allow the designers to orient them in only the directions where the strength is needed. The thinness of the plies allows designers to use only the minimum number required. The anisotropic properties of the fibers and the thin plies allow for designers to take full advantage of the fabric when designing strong and lightweight components. In the lay-up process, plies are placed in a mold of the part and conformed to the mold by either a manual or automated smoothing method. Resin is applied before, during, or after this process and when the fabric deposition is completed the resin is allowed to cure. When a part is cured, the plies should be tightly compressed to form a laminate.

Fabric sheets are produced in different structural forms such as stitched, woven, or tape. The stitched and woven forms have individual fibers joined in bundles called tows which can have cross-sectional geometries of varying shapes on the order of millimeters in diameter. The tape form is a flat sheet of parallel fibers that has been pre-impregnated with resin (pre-preg). Pre-preg tape composites are not applicable to this research because there is no stitched structure to manipulate, just resin holding the sheet together. The mechanism for deformation of tape composites is controlled by the resin binding the tows together which forces the tows to break the resin binding when severe double-curvatures are encountered on a mold. Woven or "crimp" fabrics are designed with tows that cross over and under each other throughout the fabric. The weave gives the fabric ply structure while allowing conformance to mold surfaces. These tows are typically perpendicular to each other in direction. Tows that follow the length of a fabric sheet or roll are in the warp direction. Tows that align with the width of the fabric are in the weft direction. When a tow deviates from a linear path to pass over or under a perpendicular tow, the angle of the tow off of the plane of the fabric surface is known as the crimp angle. Crimp fabrics are available in both dry and pre-preg form.

Non-crimp fabrics have no crimp angle because the tows do not pass under or over each other. The plies are given structure by a thread stitched around the tows as illustrated in Figure 1. Non-crimp fabrics are typically built from one or more unidirectional sheets of tows where all of the tows are arranged parallel to each other. These unidirectional sheets can be stacked on top of other sheets at varying angles and stitched together. The combination of anisotropic sheets stacked at varying angles allows the laminate to exhibit the quasi-isotropic characteristic of strength in multiple directions. The other use for the arrangement of one sheet perpendicular to the previous is to give the ply additional structure so the tows do not loosen or fall apart. If this arrangement is used, then the percentage of tows in one direction will be greater than the other direction. An example would be a unidirectional fabric with 90% of the fibers in the warp direction and 10% in the weft direction. The purpose of this fabric is to produce a product with anisotropic mechanical properties because the loading is known to take place on the axis of the unidirectional tows.

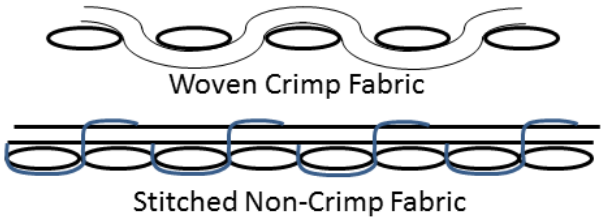

Figure 1. Crimp and non-crimp fabric.

The wind turbine industry, which is the focus of this study, uses non-crimp fabrics in every component of the blade. Manufacturing

methods for wind blades have been adapted from established methods in the boating and aerospace industries. The difference is that wind blades have a relatively low value per-weight as compared to products in other industries that utilize composite materials. To compensate for this, blade manufacturers have used low cost materials in the construction of their products. The cost of non-crimp E-glass is in the single digit dollars per kilogram, which is the lowest range for composite fabrics. Other types of fabric like carbon fiber are also used but typically only in pre-preg tapes. This is because the mechanical properties of carbon fiber rely heavily on the linearity of the fibers, which only preparation as a pre-preg can provide. These types of fabrics are an order of magnitude more expensive than the normal E-glass.

The design of a blade employs a safety factor that accounts for variation in material properties that are introduced during manufacturing. The likelihood for defects is exacerbated by poor control of the fiber deposition process due to reliance on manual manipulation of the fabric. When a fabric ply is placed into a mold it is conformed into the proper shape by manual manipulation. At times the workers must exert substantial force in order to get the fabric to lie smoothly. The likelihood of a manufacturing defect increases significantly in areas that have many plies. These areas correspond to sections of the blade carrying the most loads and therefore, are critical regions that ensure the integrity of the blade during its life cycle. These are the spar cap, which is a section on the order of 1-6cm thick (around 70-80 plies at the thickest) that runs the entire length of the blade to supply bending stiffness, and the trailing edge, which is up to 1cm thick (around 10 plies) along the length of the blade and has extreme geometry. Major changes in curvature produce these extreme geometries that force the fabric to the extents of its ability to conform to a mold surface. The fabric lay-up in these extreme geometry areas must be carefully guided so that defects are not created.

Potential defects introduced during fabric deposition correspond to deviations of a ply with respect to the mold surface or previous layer. When fabric deviates from the mold surface or previous layer and is then infused with resin, waves or wrinkles can form in the final laminate. A wave is typically characterized by a span over height ratio called the aspect ratio (AR) that can be used to determine if it is out of tolerance. A wrinkle is a defect in which the fabric has doubled over itself and is never allowable. Illustrations of these deformations can be seen in Figure 2. Smoothing performed by operators is intended to remove all waves and wrinkles. Once a defect occurs, the current process relies upon the ability of an operator to recognize that smoothing needs to be performed in that region. The process of smoothing a ply can be inconsistent and unpredictable when performed manually. The inconsistency and unpredictability in fabric deposition are primary reasons why the design must include a substantial safety factor. It would be beneficial to wind blade manufacturers to reduce the safety factor because of the weight penalty that comes with it. If a part is to be designed to overcome a certain level of manufacturing problems, then it must be made stronger, which equates to a larger, heavier part. In the wind industry component weight is of utmost importance. Lighter blades are able to be more efficient because they have lower inertial mass. Lighter blades also allow for the reduction of weight in the nacelle because it has to support less rotor weight and less stress on the motor bearings. It follows that the tower and foundation could be built less robustly due to weight savings throughout the turbine. All of these reductions lead to significant cost savings in turbine construction. Safety factor and weight reduction could also lead to blades of the same weight that are longer and are able to generate equivalent electricity in lower wind speeds. This would also be a major benefit to turbine manufacturers who could provide increased power output at the same weight. Additionally the blade manufacturer would see a major cost benefit in labor savings due to less rework and a reduction in scrapped parts.

To improve process control (i.e., process capability), we need greater consistency and predictability in fabric deposition. This translates to reducing the amount of direct manipulation of the fabric by the operators by implementing automated methods to some or all areas of fabric deposition. Automated processes could provide operators with pre-fitted

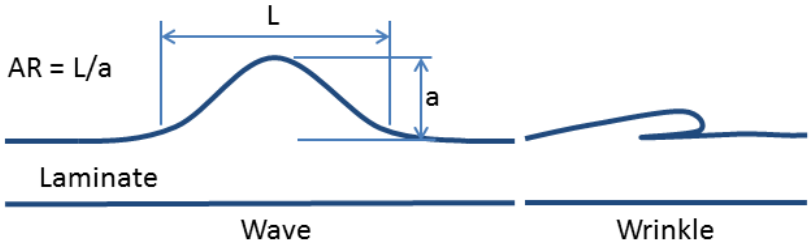

Figure 2. Out-of-plane deformations: a wave and a wrinkle.

plies for the specific mold geometry or deposit plies without human intervention.

During the fabric deposition process, bolts of two-dimensional non-crimp fabric are unrolled onto the mold surface or the surface of the previous ply, secured in certain locations, and smoothed by hand until full conformance (i.e., no defects) is achieved. The act of smoothing the fabric produces an effect called shearing. Shearing is caused by fiber tows sliding past one another as they conform to the mold. Shearing of non-crimp unidirectional fabrics has limits similar to woven fabrics due to the stitching between the warp and weft cross-tows. The relationship of the warp tows, weft tows, and stitching can be modeled as a pin-jointed net (Potter 1979). This model has been used for both crimped and non-crimped fabrics. In this model the fabric is represented as a set of deformable unit cells (i.e., squares). Each intersection of the warp and weft tows creates a vertex of a unit cell that is pinned by the stitching. The pinned intersections allow the sides of the unit cell to rotate about them. Shearing causes the angle between the sides to change. The pin jointed net model has been shown by Potter to be a good representation of fabric draping. Potter suggested two types of unit cells could be possible: one with unit cells that have inextensible unidirectional fibers and one where all fibers are inextensible. If the fibers are assumed to be inextensible then the length of the inextensible sides of the unit cell must remain constant. The unidirectional inextensible type of net preserves the initial fiber tow spacing at all points along the path of the fabric, which conserves the volume of the unit cell as shown in Figure 3 (*a*) and (*b*). This model assumes that there is some amount of tow slippage at all levels of shear because the length of the cross-fibers of the unit cell must increase. The model that assumes all fibers are inextensible allows the fiber spacing to change because the length of all four sides of the unit cell must remain constant. Figure 3 parts (*c*) and (*d*) depict the narrowing of the unit cell in the x_2 direction.

As the shape of the unit cell changes, the angle between the weft tows and their original orientation perpendicular to the warp tows proportionally changes. This angle of the weft tows from the perpendicular position is known as the shear angle (α). Assuming a completely inextensible model, the shear angle decreases from α = 90° causing the sides of the unit cell to draw closer together. The shear angle in the Tucker model decreases with the increase in shear displacement, c, however, to relate an increase in shear displacement with an increase in shear angle the shear angle will be measured from the initial position of the x_2 direction fiber as shown in Figure 4. Therefore, the initial state of shear angle will be α = 0°.

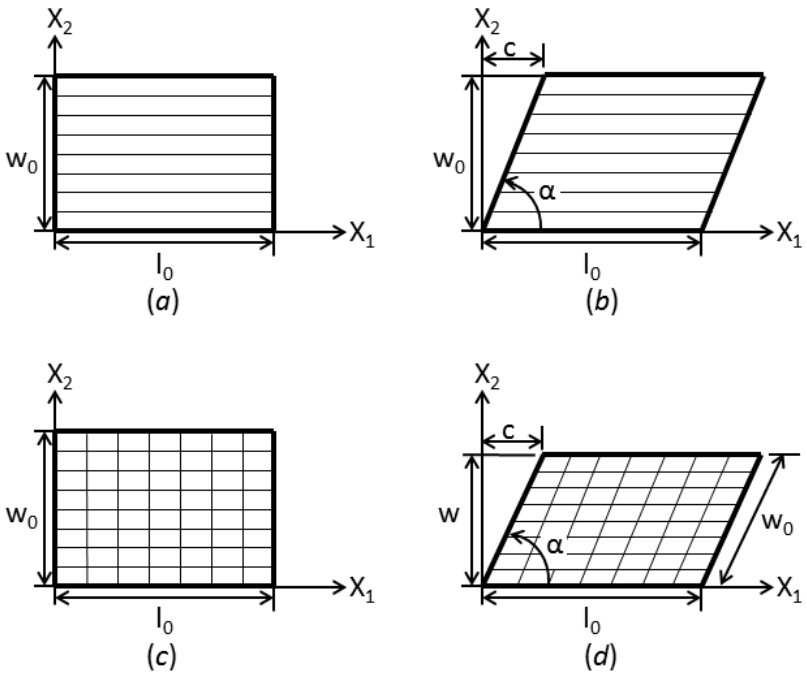

Figure 3. In-plane shear deformation of a pin-jointed net unit cell. (*a*) Original configuration of a unidirectional inextensible fabric and the (*b*) sheared configuration with conserved tow spacing. (*c*) The initial unit cell for a fabric that is inextensible in both directions and *(d*) the sheared unit cell with reduced tow spacing. Shear angle as it is measured by Tucker is represented by α. (Gutowski 1997)

The fabric tows begin at a fixed width and spacing. Shearing compression causes both the tow width and spacing to be reduced. As the tow width reduces, the cross-section shape of the warp tows are compressed from a flattened oval to a more narrow circular shape. When the minimum tow width has been reached, the maximum shear angle has been reached. This maximum shear angle is known as the shear locking limit. If shearing proceeds beyond this limit, the fabric has no space to condense further and therefore must deviate from the mold surface. At this point a wave or wrinkle is formed off of the mold surface. The shear locking limit is completely dependent on the fabric's characteristics such as tow weight, stitching type, and tow spacing.

Shearing can be distinguished by the direction in which it occurs in the fabric. Shearing in the warp (number one) direction is defined by the warp tows remaining parallel to each other while the weft

cross-tows follow variable paths. Shearing in the weft (number two) direction is defined by the cross-tows staying parallel to each other while the warp tows follow segmented paths.

Shear angle is dictated by the difference in distance travelled over the mold by neighboring tows. Each individual tow follows a unique path-line over the mold. On a flat or single curvature mold the distance traveled by neighboring tows is equal. When a three-dimensional geometry is encountered, some tows must travel a longer distance than their neighbor. This path-line difference induces a shear angle proportional to the magnitude of the displacement as illustrated in Figure 4.

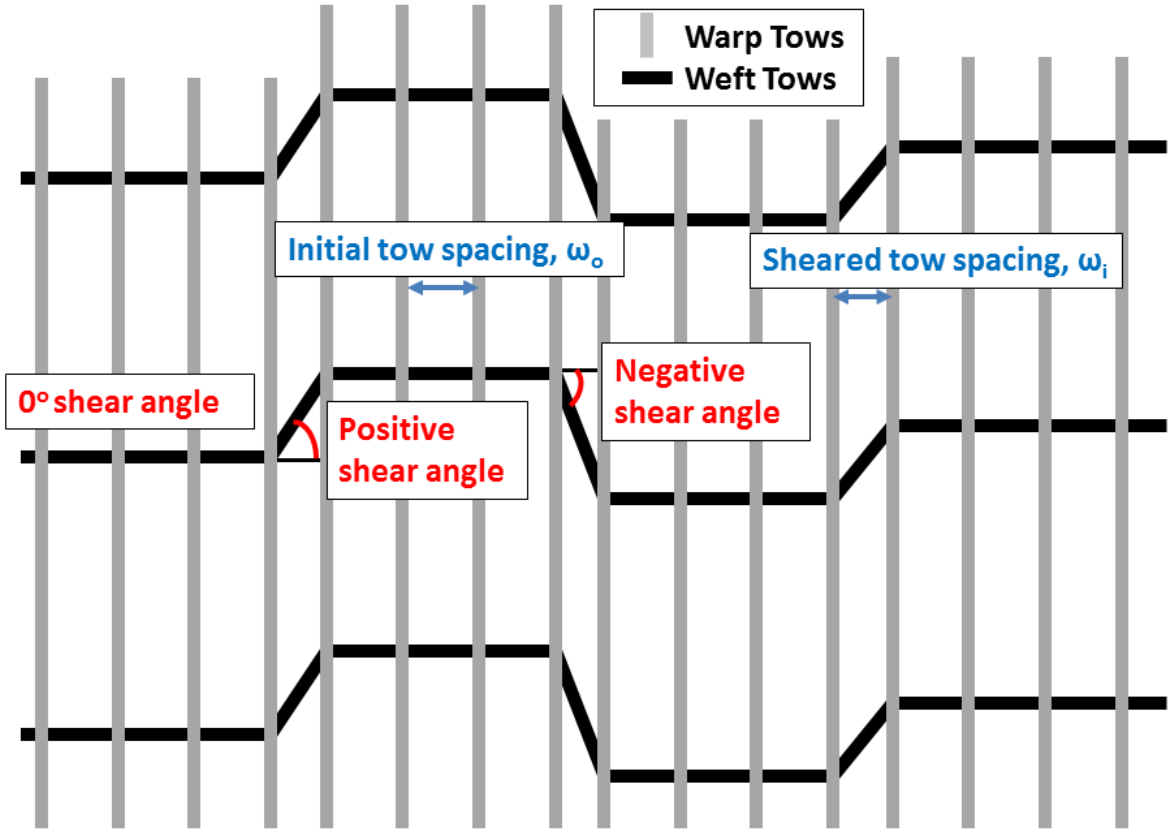

Figure 4. An illustration of a shear angle distribution. The shear angle is depicted as it is measured in Meng's (2012) software.

As the fabric is smoothed over a three-dimensional mold with multiple curvatures, the distribution of shear angle will change. The smoothing of the fabric begins at a set place called the seed position which can occur at any point on the mold. At this position the fiber orientation and shear angle of the fabric are constrained on a line either by hand, with a clamp, or by tacking the ply to the previous ply. After the constraint is applied the shear angle distribution at the seed line is locked in. A virgin fabric

will have a constant shear angle distribution of $\alpha = 0°$ at the seed line since no shearing has taken place. The fabric is then smoothed away from the seed position forcing the fabric to shear. A simple doubly curved mold will force the shear angle to increase monotonically with the length of the mold. As the length of travel away from the seed line increases, shearing may reach a point where it will not allow fabric smoothing to continue without creating out-of-plane deformations due to the shear locking limit. A conventional lay-up fixes the shear angle across the seed line to $\alpha = 0°$, which eliminates the possibility of shearing once deposition has commenced. This limits the possibilities of shear angle distributions that are available and prevents the complete optimization of shear angle distribution in the lay-up. If a shear distribution could be induced at the seed line, the lay-up could be optimized for shear distribution and possibly improve conformance, allow for more severe of longer geometries, and prevent out-of-plane deformations. The simplest form of a shear distribution would be for a doubly curved symmetric shape of constant radius. In this example the shear angle distribution could simply be the opposite of what the final distribution is found to be. Once the shear distribution is fixed at the seed position, the fabric could then proceed to shear during deposition until it reaches the initial condition of $\alpha = 0°$ across its width and then continue to shear as normal until it reaches its lock-limit again. The inclusion of the maximum inverse shear angle distribution at the seed position could effectively double the length that the fabric was meant to travel. This would allow the fabric to be fully optimized for conformance.

Chapter 2. Related Research

Fabric Draping and Shearing

The behavior of fabric structures has been widely studied in the composites industry. The draping and smoothing stages of the fabric deposition process have been specific targets for predictive software, manual deposition methods, and automated solutions. Studies have been conducted to understand the effects of fabric stiffness, lay-up orientation, and the smoothing method on the draping process.

Computer simulation of the draping process has been used to predict the behavior of the fabric structure as it deforms to create a prescription for draping and smoothing that optimizes the fiber orientation for better mechanical properties and determines the ability of a specific fabric structure to conform to mold geometry. The resulting predictions become instructions and are passed to the operators on the floor who implement them in the lay-up process. These simulations have considered factors such as the geometry of the mold surface, the orientation of the fibers on the surface, and the interaction of fibers, tows, and stitching. Due to the complexity of the problem, researchers simplified the experimental designs and computational models by using molds that have constant curvatures and symmetric geometries. (Mohammed et al. 2000a). These simulations were followed by ones that included more complex geometries and experimental tests (Potluri et al. 2001), (Van West et al. 1991).

Tam and Gutowski (1990) proposed a fiber mapping model to optimize the paths of the fiber tows. The optimized paths were desired so that out-of-plane deformations caused during lay-up could be prevented and the fibers would be aligned so the components would have the best possible mechanical properties as shown in hemispherical draping experiments conducted by Lin(2007) in Figure 5. In this model the in-plane shear was predicted at any position based on a calculation comparing the distance traveled by neighboring tows using the Tam-Gutowski Theorem (Tam and Gutowski 1990). They assumed that if the fibers are unidirectionally inextensible then any changes in length between neighbor tows must be accommodated by shearing. It was assumed that the fiber tows have constant spacing even while undergoing shear as in the unidirectional inextensible unit cell model. Tucker(Gutowski 1997) found that the constant spacing assumption of the Tam-Gutowski Theorem did not hold for unidirectional fabrics based on experimental results. Tucker posited that unidirectional fabrics must undergo an intermediate amount of slippage that was less than that proposed by Tam and Gutowski but greater than the completely inextensible model.

Further research on draping models focused on the completely inextensible unit cell. Unlike Gutowski's unidirectionally inextensible assumption, the area of the unit cell is not conserved in this model, so the fiber tow spacing is allowed to change. A pin-jointed net model allows adjacent sides of the unit cell to rotate far enough to be coincident with each other, turning the unit cell into a line. This assumes that in the fabric, tows have no thickness, but in reality the thickness varies greatly. As the shear angle of the cell increases, the tows (which are the sides of the cell) approach each other. Once in contact, a compressive force is required to drive them closer. If shearing continues, the compressive forces cause the fiber tows to compress together until they reach the shear locking limit.

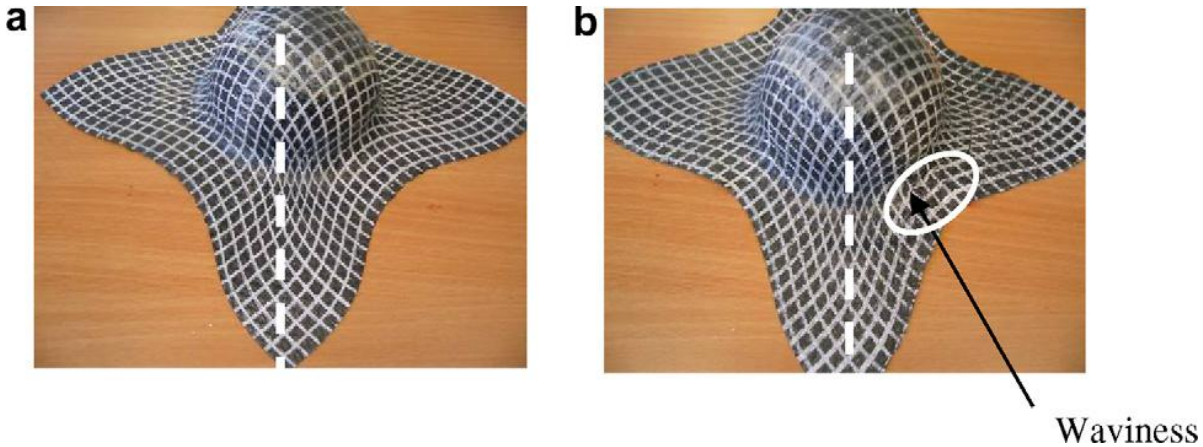

Figure 5. Experimental results of fabric shearing control from deformation using a blank and die with different boundary conditions by Lin et al. (2007). The conditions of (*a*) were optimized to produce no out-of-plane deformations like those found in (*b*).

After the maximum angle is attained, any additional compressive force from shearing results in fiber buckling and out-of-plane deformations in the form of waves and wrinkles as depicted in Figure 6. Because increased shearing forces are required to continue the compression of tows, the shearing force is shown to be directly related to the shear angle. In the pin jointed net models the shearing is distributed along the path of lowest shear force required, which provides an optimized distribution of in-plane shearing (Rozant et al. 2000), (Prodromou 1997), (Potter 1979).

Researchers have conducted empirical studies to determine the shear locking limit of different fabrics. Typically, a picture frame apparatus was used to clamp the edges of a square piece of fabric. The sides of the frame were pinned at the corners so that they were able to pivot. Opposite corners of the frame were extended away from each other, creating a parallelogram. The extension was stopped once the fabric was forced to buckle into an out-of-plane deformation. The angle of the frame at that point was equivalent to the shear locking limit (Zhu et al. 2007), (Mohammed et al. 2000b), (Prodromou and Chen 1997).

Researchers developed mathematical models of the shear locking limit to better inform designers of the capabilities and limits of fabrics based on initial conditions. Prodromou claimed that the shear locking limit of fabric could be predicted based only on tow spacing and tow size (Prodromou and

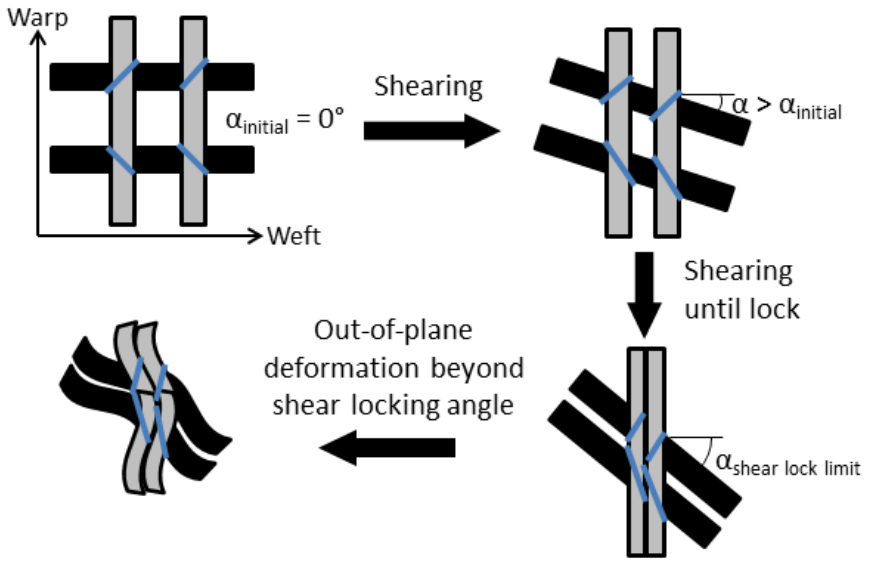

Figure 6. The process of shearing a stitched non-crimp fabric until the shear locking limit is surpassed and out-of-plane deformations are produced. Note that as shearing approaches the locking limit, the tow spacing and width is reduced.

Chen 1996). Mohammed et al. (2000b) predicted the shear locking limit of certain fabrics based on the initial properties of fiber volume fraction, unit cell dimensions, and the compression ratio of the fiber tows. McBride and Chen (1997) included the initial tow width, initial tow spacing, fabric thickness, fiber diameter and the number of filaments per tow to model the effects of shearing. They developed a mathematical solution relating those initial conditions to the shear deformation. They conducted experiments in which several types of fabric were sheared and the shear angle, tow width, and tow spacing measured with a stereomicroscope, digital camera, and image analysis software. Fabric thickness was measured with a micrometer. These experiments confirmed their mathematical solution. They showed that shearing significantly altered the geometry of the unit cell which caused the fibers to compact together as the tow spacing and tow width reduced (Figure 6) which caused a high variance in fiber volume fraction. Extremely high fiber compaction may result in limited area around each fiber for resin wetting and variability in fiber volume fraction. Therefore, the research performed by McBride and Chen suggests that in areas of very high shear angle and tow compression, there is likely to be reduced volume fraction and reduced mechanical properties.

Wang et al. (1999) used a pin jointed net model to predict the draping process based on different seed positions, constraint methods, and fabric orientations. The goals were to prevent out-of-plane deformations due to surpassing the shear locking limit, have the greatest area of minimum shear angle, and satisfy the tolerances on fiber orientation. Their experimental results agreed well with the simulations, which provided substantially different draping patterns depending on the initial conditions. They encountered tow slippage, which he attributed to the magnitude of the shear angle. They also suggested “pre-stretching” the fabric prior to deposition as a means to prevent out-of-plane deformations, but completed no simulations or experiments to support this.

Lai and Young (1999) argued that the inextensible pin jointed net model is not completely comprehensive because it does not include fiber slippage. In reality the segments of the unit cells are not connected by pins but are constrained due to the friction of the stitching or weave. Lain and Young proposed the inclusion of a slippage model that improved the results of the deformation simulation. Bickerton (1997) also showed that fiber slippage does occur, especially in areas of high shear. The DRAPE model used in their experiments assumed that fiber slippage was negligible, but experimental results revealed that the software had over-predicted shear levels in areas where the shearing forces were strongest.

Other researchers have proposed that a simulation of the fabric as a continuum with anisotropic elastic mechanical properties will provide an accurate model of the draping characteristics. Dong et al. (2000) developed such a model that considered the elastic modulus of the fabric, friction of the fabric, deposition speed, mesh size, and clamping force to determine the effects of the draping pattern. Lin et al. 2007 used a mechanical finite element model for simulating the impact of the draping configuration on the mechanical properties of the laminate.

Hancock and Potter (2005) suggested that inverse drape modeling can be used to evaluate the manufacturability of a design. This method used the draping capabilities associated with a specific type of fabric as an input to design. They suggested that small design alterations could result in substantial improvements in the ability of the fabric to conform to the mold.

Hancock and Potter (2006) also used a kinematic drape model to improve the hand lay-up process. The intuitive approach to fabric deposition used by workers can result in non-optimized shear distribution, which causes out-of-plane deformations. This model employed a pin jointed net representation of the fabric to create better in-plane shear distribution maps. These maps were used to create detailed instructions for the workers that described the order of smoothing areas of the fabric. In this way the ad hoc approach used by workers was replaced by explicit instructions.

All of the research presented thus far primarily addressed the development and validation of fabric draping simulations. However, the relationship between these simulations and the lay-up process is not well defined. The precise knowledge of in-plane shearing distributions was not connected to the manufacturing process. Many of the shear mapping software validations were successful but limited to vacuum formed testing, which cannot be used in many areas of the composites industry. Hancock and Potter (2006) attempted to develop a strategy for guiding workers with a lay-up plan. However, the consistent implementation of process controls from simulation to shop floor practice can be met with varying success. Even with comprehensive lay-up instructions it remains difficult to produce consistent parts by hand and results may further vary from worker to worker. Consistent lay-up of fabric such that out of plane deformations are eliminated will require much more rigorous process control in the form of automated fabric deposition and smoothing. An alternate approach would be a process which creates deterministic fabrics through an automated means. A deterministic fabric is one that will conform to the shape of its intended mold with little or no intervention of workers. Both

of these solutions could provide a means to control the deformation of fabric without having to extensively instruct operators.

Automated Fabric Deposition

Manual fabric deposition can result in several problems. The naïve approach used by fabric lay-up workers can cause non-optimized in-plane shear distribution, out-of-plane deformations on parts with high shearing (Hancock and Potter 2006), and especially inconsistent shear distributions. All of these issues can result in weakened mechanical properties, extensive rework, or scrapping of parts. To overcome these problems, the composites industry and researchers have explored several methods to automate all or part of the deposition and smoothing process. Unfortunately, due to considerations such as material cost, equipment cost, scalability, and processing time, many of these automated methods are limited in application.

In many of the previously mentioned research experiments, a vacuum forming method was used to create experimental samples for draping analysis. This type of fabric deposition requires no manual involvement. Fabric is suspended above a lower positive mold and an upper negative mold is lowered onto it with vacuum pressure. In this case the fabric shearing follows the path of lowest shear force required, which serves to validate the kinematic pin jointed net shearing models (Mohammed 2000a), (Potter 2002). Obviously, this type of automation would not be scalable to large components such as utility scale wind turbine blades. The infrastructure would be extremely large and a two-part solid mold cannot provide the fiber compaction required for the extremely thick laminates.

Other forms of automation common to the aerospace industry are CNC automated tape lay-up (ATL) and automated fiber placement (AFP) (Debout et al. 2011). The ATL process uses a narrow roll of pre-preg tape (e.g. 2 to 30cm wide) while the AFP process uses individual fiber tows. Both methods deposit the fibers onto a mold via a robotic head and compaction roller as shown in Figure 7. A multi-axis robotic arm provides the head with access to geometry and controls fiber orientation. The pre-impregnated resin provides tack that allows the layers to stick together during deposition. The narrow tapes/tows which do not have cross tows or stitching allow these processes to avoid some of the problems caused by in-plane shearing (Dirk et al. 2011). This process has a relatively slow deposition rate compared to hand lay-up due to the narrow tapes and using wider tapes limits the in-

plane curvature. These processes are more appropriate for single curvature laminates using high value carbon fiber. Because the deposition process is pre-programed and consistent, the scrap rate of expensive parts is reduced (AC Long 2005), (Shirinzadeh et al. 2004).

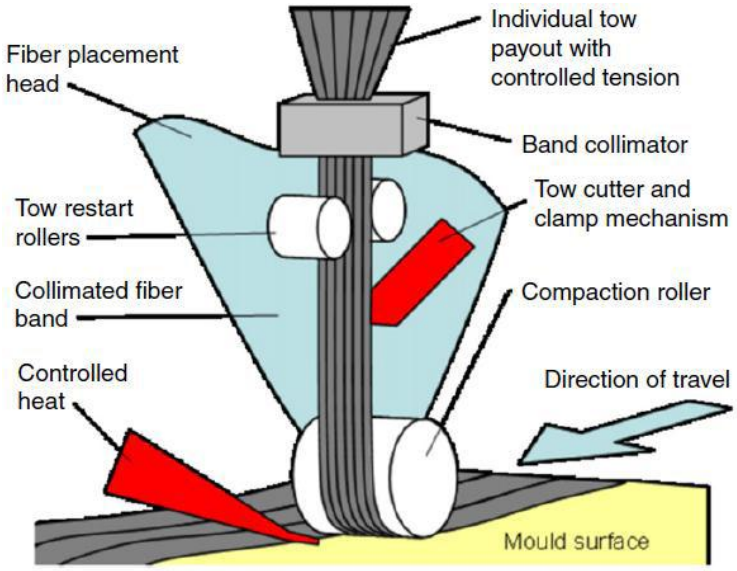

Figure 7. Automated Fiber Placement (Debout et al. 2011).

Several research groups have investigated the feasibility of an automated work cell for handling and deposition of broad (e.g. >30cm wide) composite plies. Several handling methods were tested to transfer the fabric to the mold surface. The fabric was then draped over the mold using a robotic arm and smoothed using various tools that mimicked those used in hand lay-up. These tools adequately formed the plies to the mold, but gave no consideration to guiding the in-plane shearing distribution (Buckingham and Newell 1996), (Ruth and Mulgaonkar 1990).

Kordi et al. (2007) also employed a robotic arm system for their automated fabric deposition device. This device used a four segment conformable end-effector to transfer large plies onto a mold. This method was limited by the ability of the four end-effector segments to approximate the curvature of the mold. They also developed a tool head for a robotic arm which could carry two types of rollers for smoothing the plies.

Patents have also been issued for several types of conformable head multi-axis broad fabric placement machines. These machines were designed to smooth the fabric as it was deposited onto the mold off of the roll. This type of device has advantages in deposition rate and consistency, but just as the previous smoothing devices, do not account for in-plane shearing. These devices would be appropriate for large objects with smooth, large radius curvatures.

Potluri and Atkinson (2003) conducted experiments to quantify the effects of material handling on the in-plane and out-of-plane deformations of the fabric. This was useful for predicting the draping characteristics of a fabric deposited onto a mold.

Rudd et al. (1999) developed a tow placement device for creating unique 2D plies that would have the tow orientation and spacing designed for deposition to specific molds. This was an application of the deterministic material approach to manufacturing. The machine would combine the AFP idea of placing a single tow or several tows at a time, but simplify it to a two dimensional plane. The optimized fiber orientation and spacing for fabric on a specific 3D mold were generated by software and then translated into 2D. This process would allow plies to be created off-line and prepared with the process controls for governing the in-plane shearing distribution imbedded in them. The plies were held together by the application of a tackifying agent during the fiber placement. After the plies were deposited and smoothed onto the mold, the problem of high in-plane shearing causing undesirable deformations was eliminated. Obviously, this type of deterministic ply creation would be limited to smaller objects due to long cycle times.

Robotic material handling and smoothing may be able to provide a means for consistently produced lay-ups, but none of those methods were able to address the shear deformation mapping described previously. Even with the information available from shear mapping programs, the only automated way to implement them is through lay-up methods like vacuum forming which mimic the shear distribution process of the program, otherwise the shear mapping process controls must be passed to the lay-up operator which will produce inconsistent results. The idea of creating in-plane shear optimized fabrics by individual tow placement does provide a deterministic material approach to the process of controlling the shearing distribution without worker intervention. However, this idea is not well suited for the production of extremely large scale objects like wind blades which use very large plies of unidirectional non-crimp fabric. A more pragmatic application of the deterministic material approach to process control would be to change the shear angle distribution of any non-crimp broad loom fabric to the desired alignment prior to deposition. Research has been conducted into using shear angle mapping to guide a robotic deposition head by Magnussen (2011). This method would allow a deposition head to approximate a curved fabric path by using incremental discrete 2D “shifts” in the weft direction. This process could provide a pre-sheared unidirectional fabric that requires minimal smoothing by operators. The fabric deposited by this device would be deterministic in nature because it would already be formed to a 2D representation of the 3D part geometry. This

process addressed curvature perpendicular to the warp direction of the fabric as shown in Figure 8. The shifting process does not, however, address process controls for fabric that needs to conform to multiple curvatures from all directions. To employ the deterministic approach for controlling the final shear angle distribution, the fabric must be manipulated at the tow level. The shear between neighboring tows across the width of the unidirectional fabric must be controlled. An automated device providing this control must manipulate individual or small groups of tows to create a desired level of shearing between them. Currently, no such manipulation device exists and preliminary work must be conducted to understand the process requirements and capabilities. One requirement is that it must scale to an industrial level while providing acceptable results. Research in this paper has been conducted to determine the feasibility of such a device and the effects that approximation for industrial scalability would have on the process control.

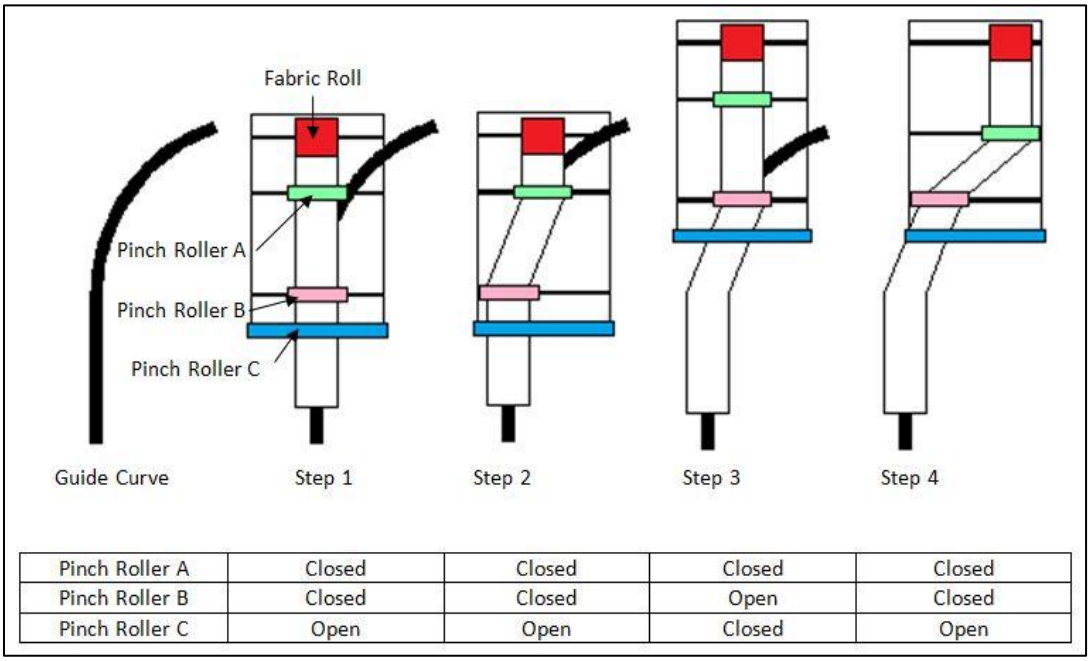

Pinch Roller A	Closed	Closed	Closed	Closed
Pinch Roller B	Closed	Closed	Open	Closed
Pinch Roller C	Open	Open	Closed	Open

Figure 8. The process of a conceptual automated "shifting" head (Magnussen 2011).

Research Problem

The key to improving the fabric deposition process is to exploit our knowledge of fabric shearing to ensure conformance of plies to the mold. In current practice, a designer knows the capability of a fabric in terms of its shear locking limit. The designer specifies the path that the fabric follows within that limit. Currently, the shear locking limit is calculated by programs that model fabric draping from a single point, line, or combination of lines at the seed position where the fabric is initially deposited

and smoothed away from. The initial condition at the seed position is that of $\alpha = 0°$. Smoothing away from this point is simulated and when the shear locking limit is reached the simulation ends unless the fabric is cut using a dart cut, the seed position is changed, the fabric is changed, or the mold design is changed. The knowledge of the shearing properties must then be passed to the operators in the form of work instructions. The designer relies on the worker to use the specified seed position and perform the smoothing operation correctly. As stated previously this objective is met with inconsistent results especially when simulated fabric deposition is unavailable. The workers often perform the operations naïvely, without specific knowledge of the shearing properties other than previous lessons learned. Sometimes the designer is limited by manufacturing capabilities or fabric characteristics, so the safety margin must be increased or the part design altered to compensate. If a deterministic shearing distribution were incorporated into the fabric itself, the process would be more consistent. An automated solution would allow the shear angle distribution to be passed onto the work floor without passing through a naïve process. Automating all or part of the fabric deposition process would achieve greater consistency and improve process capability.

The simplest method for imbedding a deterministic shear angle distribution into the fabric would be to shear the fabric prior to deposition while it is in a two-dimensional state. This can be accomplished by shearing specific tows in the ply to create an optimized shear angle distribution. A device that could accomplish this task would require the ability to grasp specific tows and precisely pull them into the correct displacement relative to other tows. It would also be useful for the device to use a minimum number of grasping points to produce the shear angle distribution. A smaller number of grasping points would minimize the number of axes of control, reducing the cost and complexity. However, a smaller number of grasping points would reduce the resolution of the shear distribution approximation. A new method for automated fabric pre-shearing that imbeds deterministic shearing process control into the fabric would minimize deformations caused by workers, allow greater freedom in blade design, and provide a pathway for more advanced automation in the future.

Research Questions

For automated deterministic fabric pre-shearing to be implemented there are several important questions that must be answered to determine the feasibility of this method.

1. Can fabric plies be consistently produced with imbedded shear angle distributions?
2. Will an approximated shear angle distribution reduce out of plane deformations when a ply is smoothed into the mold?
3. What effect does changing the resolution of the shearing profile approximation have on conformance to the mold surface?

Approach

Using the fabric draping simulation model developed by Meng (2012), we find the necessary tow displacements that allow for the full extent of the fabric shearing to occur in order to prevent downstream out-of-plane deformations. This includes a designed shear angle distribution at the seed position. The method places each tow on a path-line over the mold starting from a common seed line, measures the difference in path-line length between neighboring tows, and equates that with a shear angle distribution. If a mold design causes the fabric to surpass its shear locking limit, the program generates an idealized shear angle distribution. This idealized solution spreads higher shearing to areas of previously low shear angle, which includes pre-shearing tows at the seed position. By distributing higher shear upstream from the areas approaching shear-lock, the useful length of fabric is increased. The pre-shearing is then equated back to tow displacement. This simulation provides the magnitude of displacement for each individual fiber tow in a fabric. This creates a tow displacement profile that can be implemented on the fabric by physical manipulation in 2D.

The tow displacement profile shows the necessary displacement length for each tow. In large-scale applications such as wind energy, fabrics can contain over 100 tows across their width. Physically implementing a tow displacement resolution at the individual tow level is not scalable due to the number of control axes that would be needed. Therefore, an approximation is required. For an industrial application of the proposed method it would be advantageous to reduce the number of fabric grasping points to the absolute minimum. To do this requires that individual tows be grouped together and displaced the same amount by a single grasping device.

To simplify the pre-shearing process to its most basic form, the shearing was limited to discrete manipulations. Discrete manipulations induce a constant shear angle over the entire length between neighboring tows. This creates a constant approximated displacement profile in the warp direction. After the fabric undergoes this manipulation it can be placed in the mold it was designed for as if it were a normal fabric ply. The ply is clamped at the seed position and smoothed away from that point. After the deposition is complete, the investigation of conformance to the mold shape can commence.

D

Th

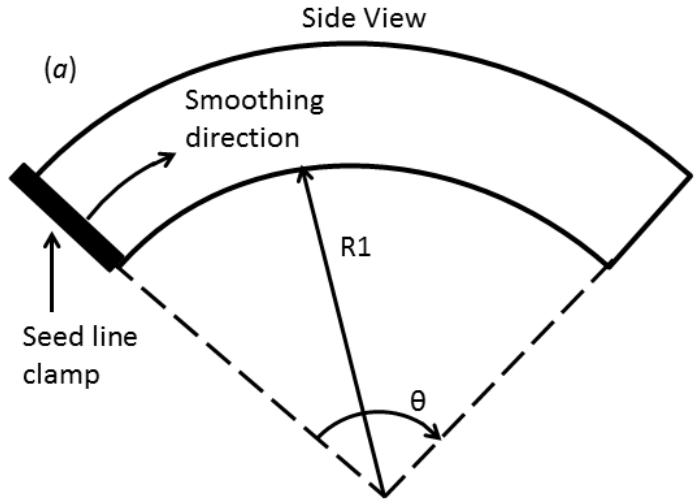

ed

ıe.

ng

s.

Figure 9. Simulation parameters for a doubly curved mold.

5. Deposit and smooth the fabric into the mold.
6. Laser scan the surface of the fabric.
7. Analyze the surface meshes of the fabric in RapidForm.

Draping Simulation

The draping simulation developed by Meng (2012) was used to generate an optimized shearing solution using fabric "pre-shearing" for a doubly curved mold. The simulation is limited to molds having a symmetric, interior, toroidal section. The toroidal section is defined by a convex major radius and a concave minor radius. This arrangement was chosen because it resembles the form of a wind turbine blade spar cap mold. It also allows for simple smoothing because the cross-section geometry remains constant. The mold parameter inputs to the program are: major radius (R1), minor radius (R2), width (W), angular distance (θ), seed position ($\theta_{seed\ line}$), and fabric end position (θ_{end}) as shown if **Error! Reference source not found.**.

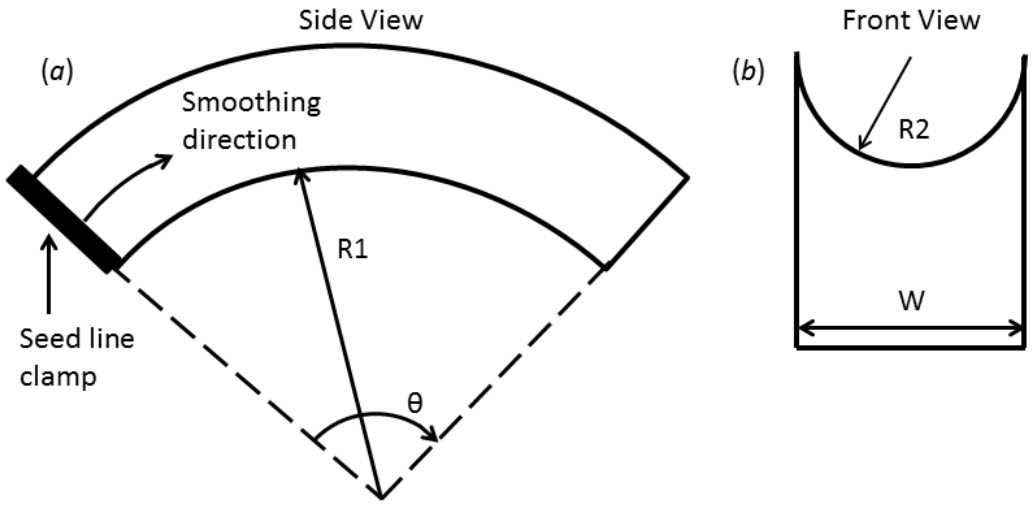

Figure 9. Simulation parameters for a doubly curved mold.

The inputs for the fabric initial conditions are: tow width, fabric thickness, shear locking limit, and number of tows. Using these parameters, the simulation generates a lay-up using the naïve lay-up method (Figure 10(*left*)) and another, deterministically optimized shear angle distribution lay-up using a pre-sheared fabric (Figure 10(*right*)).

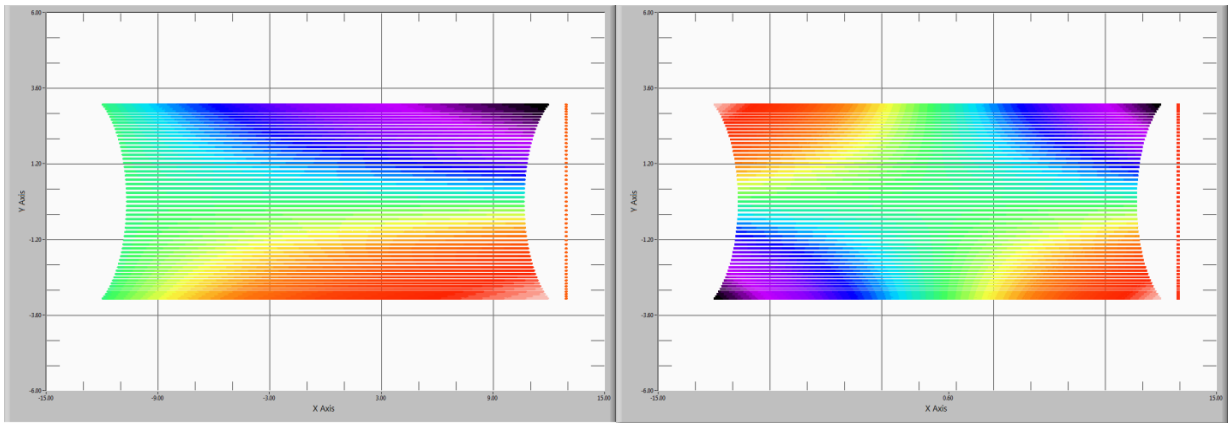

Figure 10. A color map of the shear-angle for an un-sheared fabric deposition with a maximum shear-angle of 54°(*left*). A color map of the pre-sheared fabric deposition with a maximum shear-angle of 34°(*right*). The color gradients are on a relative scale.

The optimized shear angle map uses the lay-up that produces the lowest maximum shear angle. The optimized solution assumes that there is a shearing distribution at the seed position. The only way to generate shearing at the seed position is to pre-shear the fabric before it is deposited. Pre-shearing consists of manipulating the tows in 2D to create a constant shear angle between the entire lengths of

neighboring tows. If the correct amount of shearing is induced in the fabric, then the resulting shear angle distribution would be optimized as shown in Figure 10(*right*). Because shearing can be equated to a difference in distance traveled along the path-line, the tows can be displaced relative to each other to produce the pre-shearing effect. An example of constant shear angle distribution for pre-shearing is shown in Figure 11. In this example the shear angle decreases towards the center of the ply. Since the shear angle is constant between neighboring tows it can be equated to a difference in displacement length at the end of the ply. The program represents this displacement length difference as a table called the pre-shearing profile. This profile prescribes the displacement length required to create the appropriate shear angle for every fiber tow. The tows can then be physically displaced to match the profile.

Shearing Apparatus

The apparatus used to pre-shear the fabric has a minimum resolution of four tows per group. Four was chosen as a mid-range between a single tow and an eight tow resolution. The single tow would be highly impractical due to the small inconsistencies of tow width that can arise on that scale. An example of individual tow resolution is shown in Figure 12(*a*). Groupings of eight tows were also deemed impractical during a pilot study. In this study, groups of eight tows were sheared, but the shear angle induced between the neighboring tows exceeded the shear locking limit. This caused out-of-plane wrinkling and in-plane distortion of the fabric. In this case, the outermost group of eight tows remained in place while the neighboring group of eight was displaced. The high level of shearing that occurred between the neighboring tows in this pilot study was a result of the total difference in shear displacement from the outermost tow to the ninth tow being accommodated by the shearing between only the eighth and ninth tows as shown in Figure 12(*b*). This is not surprising because of the cumulative effect that grouping of tows has on the linear displacement necessary to produce the prescribed shear angle (i.e., total shear angle is proportional to the number of tows). Using the four tow groupings, the shearing device is capable of creating a stepped approximation of the tow displacement profile produced by the software as shown in Figure 12(*c*) or a stepped and linear approximation as in Figure 12(*d*). The pre-shearing process uses two sets of

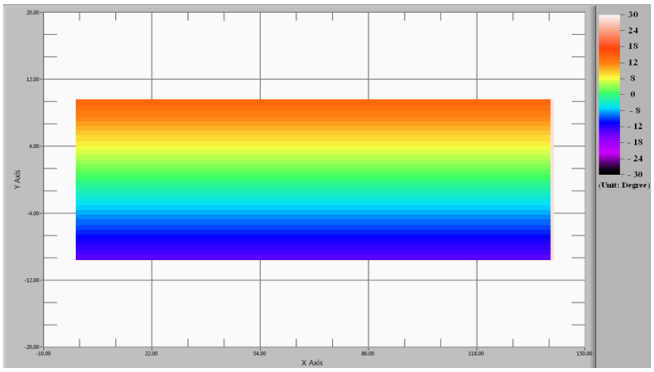

Figure 11. A draping simulation output of the constant shear angle distribution that is the result of discrete pre-shearing.

clamps. Both clamps have individual teeth that can clamp onto four tows. The teeth are positioned in slight contact with their neighboring teeth so that all tows will be covered. One clamp remains stationary and the other, positioned a distance away, is displaced a fixed distance using a controlled linear screw. A schematic of the device is shown in Figure 14 with fewer teeth than the actual device. Fabric was placed in the clamps, the set of tows that were to remain stationary were clamped on the non-moving end, and the set of tows to be sheared were clamped on the sliding end. The distance the sliding end traveled away from the stationary clamp was equal to the desired displacement between the tows clamped at either end. The pattern of clamps could be changed to reflect the prescribed tow displacement profile.

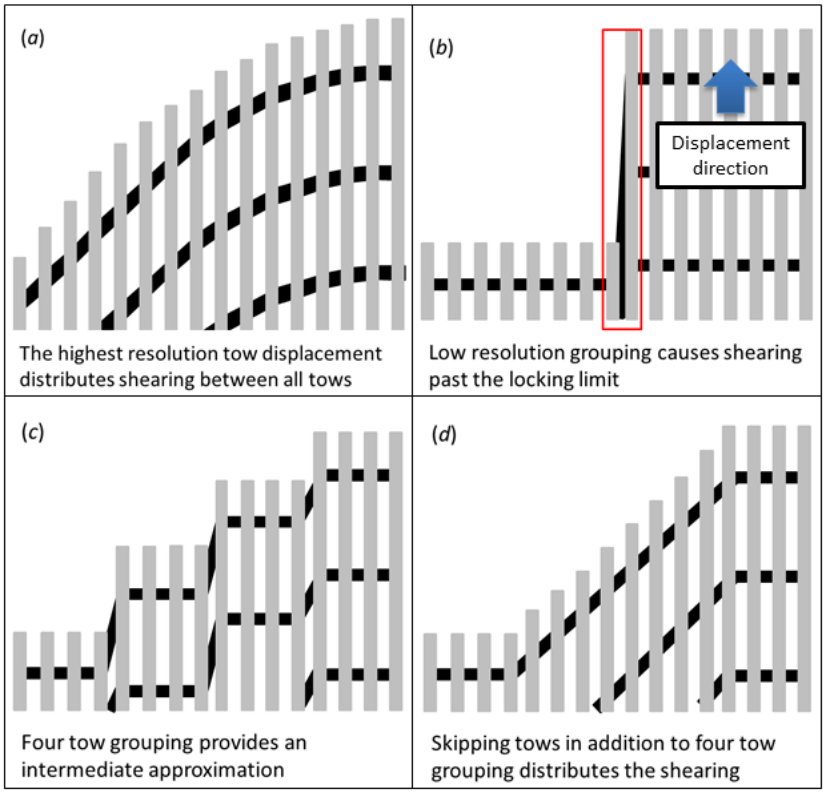

Figure 12. Tow displacement profiles for (a) individual tow resolution, (b) eight tow grouping, (c) four tow grouping, and (d) skipping tows between four tow groups.

Before the fabric was placed into the shearing device, it was cut to a length of 106.7cm (42in) in the warp direction and marked with a line perpendicular to the warp tows in three locations as shown in Figure 13. These lines provided references for measuring the actual displacement induced by the device after shearing. The clamps were separated by 81.3cm (32in). The displacement distance was measured using a linear variable differential transformer (LVDT) that produces a voltage proportional to displacement connected between the frame of the apparatus and the sliding clamp as shown in Figure 14. The voltage was measured using a standard voltmeter as shown in Figure 15. The device was designed to shear only neighboring tow groups, one tow group clamped on the stationary side, $group_{i-1}$, and the next group clamped on the movable side, $group_i$. The total shearing displacement for $group_i$ would be l_i. A consequence of this method was that all unclamped tow groups

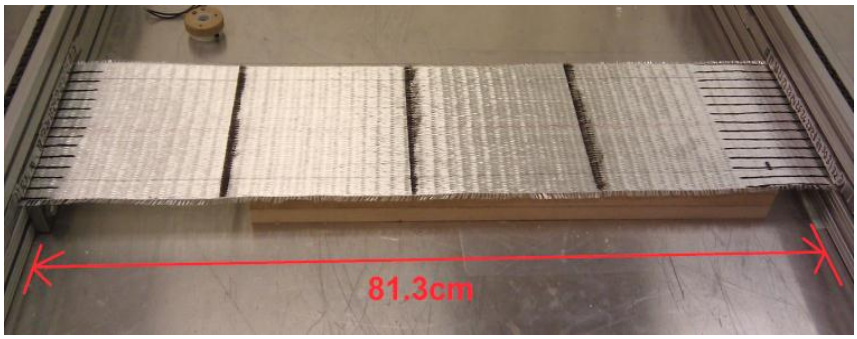

Figure 13. The fiberglass fabric placed into the shearing device after being marked with reference lines.

(*group*$_{i+1,2,3,\ldots}$) were also displaced the same amount as *group*$_i$. To compensate for this, the displacements were conducted in order from smallest to largest; the smallest displacement being *group*$_i$, the next smallest being *group*$_{i+1}$, and so on. In this way the shearing displacement of consecutive groups would be cumulative. Therefore, *group*$_1$ would be displaced l_1 then *group*$_2$ would be displaced the difference between l_2 and l_1 or Δl_2. The displacement of any tow group can be calculated as:

$$\Delta l_i = l_i - l_{i-1} \tag{1}$$

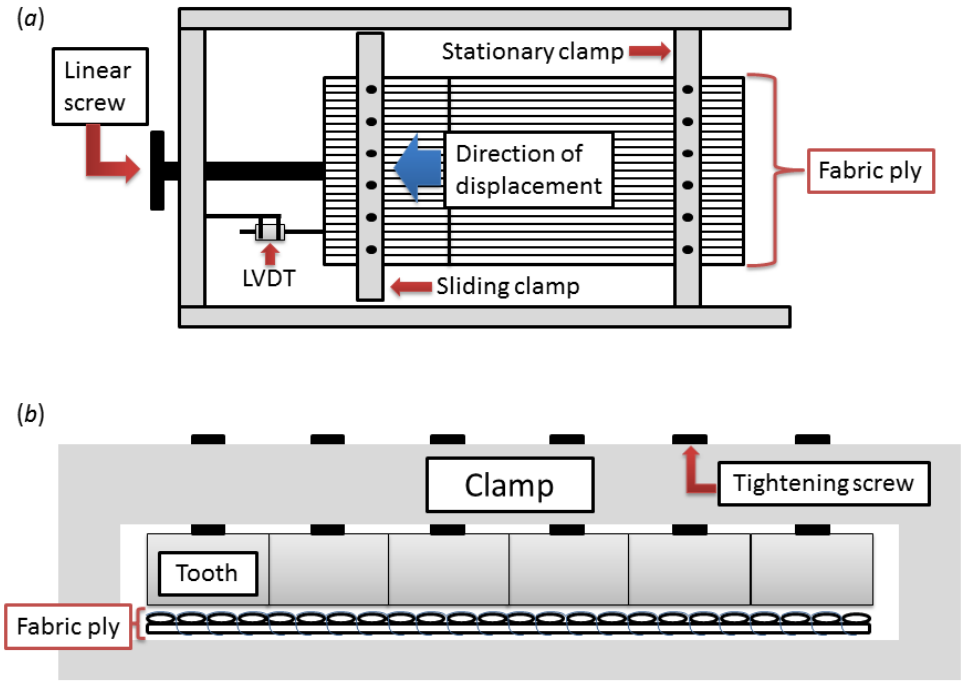

Figure 14. A simplified depiction of the shearing device. (a) The top view of the device. (b) The front view of a clamp.

After $group_2$ was sheared, the teeth for $group_3$ were tightened and the previous teeth released. The sliding clamp was then moved a distance of Δl_3. This process was repeated until the tow group with the maximum displacement distance was sheared.

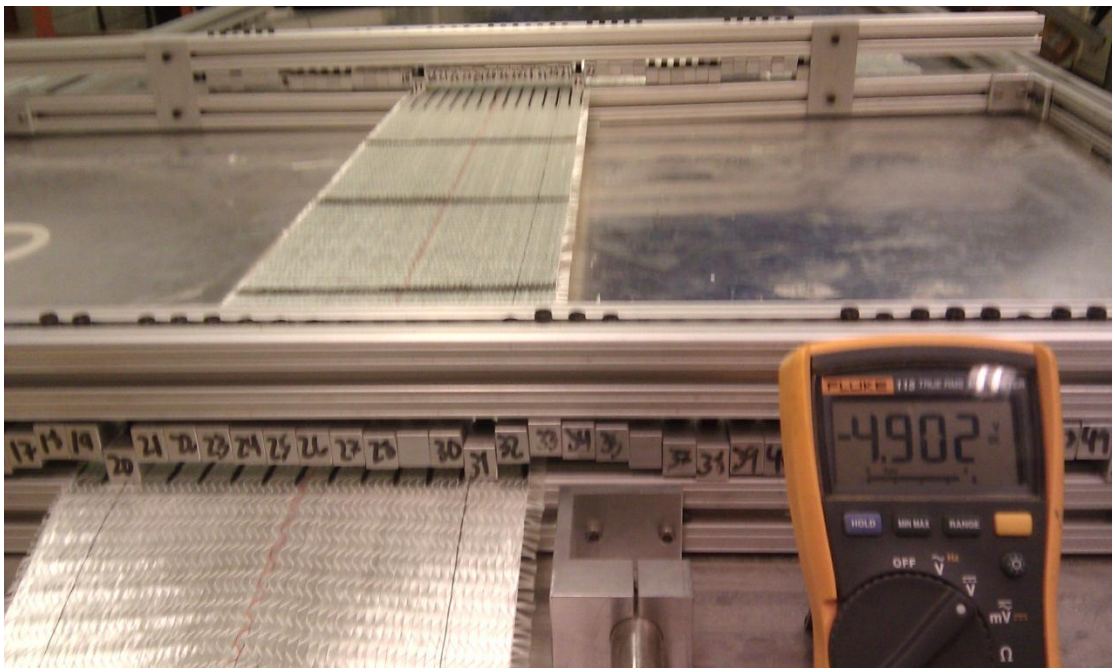

Figure 15. The pre-shearing apparatus with the moving clamp and LVDT in the foreground and the stationary clamp in the background.

Mold Geometry

A mold was created to test the fabric samples' ability to conform to a 3D geometry with significant curvature. The mold was designed with the help of draping simulation software (Meng 2012). The goal of the mold design was to create a doubly curved shape severe enough that it would force normal fabric to exceed its shear locking limit and thus create out-of-plane deformations. The shear locking limit of typical fabric used in the wind industry was found using picture frame testing. The fabric used in the experiment was a Seartex 930 g/m^2 unidirectional non-crimp fiberglass, which had 56 warp tows and was found to have a shear locking limit of approximately 45°. The fabric had 10% by weight cross-tows stitched to the reverse side to provide fabric structure. To simplify the design a symmetric mold shape was chosen and generated in the draping simulation. Figure 1Figure 9 is a diagram of the mold which is a 90° section of the inside of a torus. The relevant parameters of the fabric and mold are shown in Table 1. A 3D rendering of the mold can be seen in Figure 16.

Table 1. The draping simulation input parameters from the test mold and the initial fabric conditions.

Mold Parameters		Fabric Initial Conditions	
R1	15in	Tow width	.1395in
R2	3.5in	Fabric thickness	.03in
W	7in	Number of tows	56
θ	90°	Shear Lock Limit	45°
θseed line	0°		
θend	90°		

The parameters were input into the draping simulation and the shear angle distribution map was calculated. The results indicated that the fabric would experience a maximum shear angle of 54° at the end of the mold, far exceeding the locking limit. To verify these predictions, a 76.2cm (30in) length of fabric was tested in the mold using a clamp at the θ = 0° position as a seed line ($\theta_{seed\ line}$). The fabric was evenly smoothed over the mold beginning at the seed position resulting in two distinct wrinkles, confirming that the shear locking limit was exceeded which resulted in an out-of-plane deformation and a defective lay-up.

Figure 16. The toroidal section mold.

Shearing Relaxation Compensation

A calibration of the shearing device was performed for each fabric sample set in the experiment. It was known from initial testing that the fabric would undergo some relaxation following a pre-shearing manipulation. To account for this, the amount of total displacement was measured in three locations for each tow group after the sample was removed from the device and cut to its final size of

76.2cm (30in). Based on initial testing in the pilot study a process capability of ±3.0mm (.12in) was deemed to be achievable. Compensation for the relaxation consisted of trial and error testing. The ideal displacements were used on the initial test and adjusted accordingly until all of the displacement errors were within ±3.0mm of the prescribed linear displacement. After this level of accuracy was reached, additional samples were created for each sample group using this calibration. The measurement data collected during the calibration process served to answer research question one, which asked if it was possible to consistently produce permanent shear angle distributions on 2D fabric.

Experiment

Objective

The goal of the experiment was to determine if pre-shearing the fabric using reduced tow resolution would decrease the maximum shear angle experienced by the fabric and therefore, not produce out-of-plane deformations. To accomplish this, 106.68cm (42in) lengths of the fabric were pre-sheared as described in the previous sections and then cut to 76.2cm (30in). The purpose of cutting the fabric after shearing was to eliminate any effects that the clamps themselves had on the tow spacing and to present the fabric so that it was indistinguishable from the un-sheared counterpart. After the deposition of both the original and pre-sheared samples, a non-contact laser scanning inspection was performed to evaluate the conformance of the fabric.

Independent Variable

Experimental tests were required to address research questions two and three, which concern the effect of tow grouping resolution on fabric conformance and the presence of out-of-plane deformations. The independent variable that was controlled for this experiment was the configuration of the clamping teeth on the tow groupings. Five tow grouping configurations were proposed for this experiment. The first configuration was the closest stepped approximation to the prescribed shear profile utilizing all of the available clamp teeth individually. The remaining tow grouping patterns included tow groups that were skipped to create a linear approximation between the tows that were clamped and sheared. Table 2 defines the tow grouping patterns used in the experiment. The difference between sample sets is the spacing between clamped tow groups, ranging from 0 to 5 tow group spaces. Four replications were completed for each sample set of this experiment.

Table 2. The pattern of tow groupings chosen for comparison. For "Sample set E" the outer two tows are clamped on each side using half a tooth each and the innermost four tows are clamped with a single tooth.

Sample set	Number of tow groupings	Tow Groups Clamped													
		1	2	3	4	5	6	7	8	9	10	11	12	13	14
A	14	■	■	■	■	■	■	■	■	■	■	■	■	■	■
B	8	■		■		■		■	■		■		■		■
C	6	■			■			■	■			■			■
D	4	■						■	■						■
E	3	▒						▒	▒						▒

Dependent Variable

The dependent variables to be measured in the data acquisition and analysis phases were the out-of-plane deformations that appeared after the fabric was smoothed. The important characteristic of the deformations to quantify was severity. Several metrics were used to characterize severity:

- Average deviation of the fabric from the nominal mold surface
- Average deviation of just the deformations from the mold surface
- Frequency of out-of-plane deformations (waves)
- Average aspect ratio (AR) of the worst waves
- Lowest (worst) AR present on any lay-up
- Length of the worst waves

Draping Simulation and Profile Approximation

The draping simulation developed by Meng (2012) was used to generate an optimized shearing solution using fabric pre-shearing. The mold parameters and fabric initial conditions were input with English units as shown in Table 1. The simulation generated an optimized solution for the shear angle distribution of the fabric which reduced the maximum shear angle of the fabric to 34° as shown in the relative scale color map outputs in Figure 10(*right*). This maximum shear angle was well within the shear locking limit of 54° for this fabric therefore out-of-plane deformations would be prevented. If the correct amount of pre-shearing is induced in the fabric then the resulting shear angle distribution would be optimized as shown in Figure 10(*right*). The optimized shear angle distribution created by the simulation can be implemented by using the pre-shearing linear displacement profile that is output by the program as shown in Figure 17.

Because the pre-shearing device had a minimum resolution of four tows per group, the pre-shear profile displacements were divided into groups of neighboring tows. The average displacement of each group was used for the displacement distance except for the first group which remained stationary at zero displacement. Because the mold was symmetric, the pre-shear profile was mirrored across the width of the fabric. Therefore, the tow groups on opposite sides had the same displacement length. Tow groups that have the same displacement can be paired during shearing. This allowed the tow groups on opposite sides to be clamped and sheared simultaneously as shown in Figure 18.

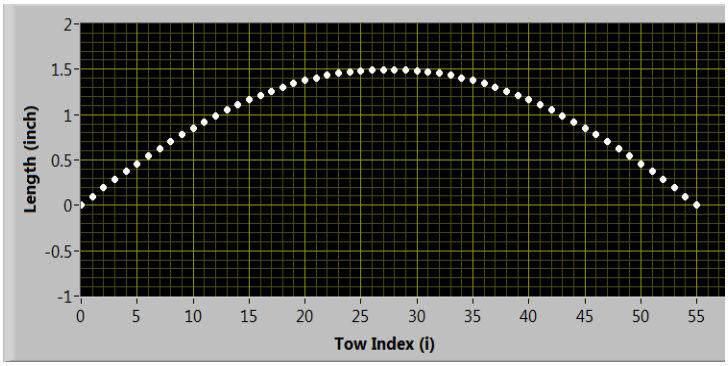

Figure 17. The tow-displacement profile required to pre-shear the fabric produced by the fabric draping simulation.

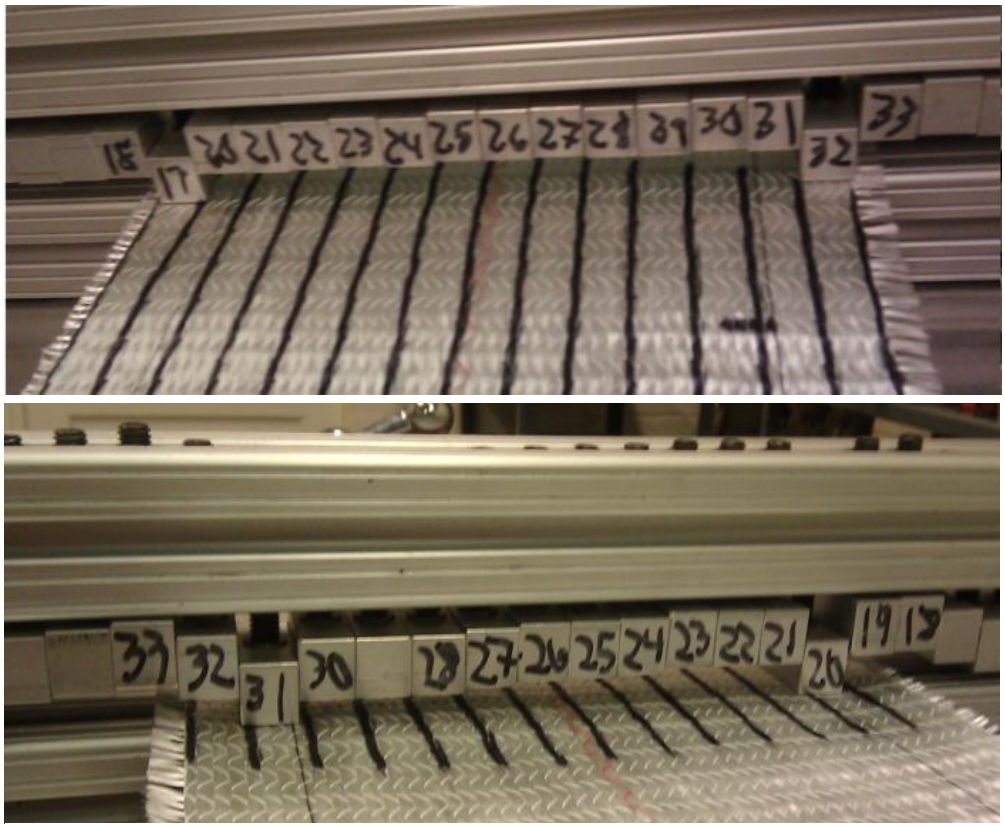

Figure 18. Prior to the first displacement the outermost tow groups were clamped on the stationary clamp(*top*) and the adjacent tow groups were clamped on the sliding clamp(*bottom*).

Pre-shearing Process

Figure 20 shows the first three steps of the pre-shearing process. Starting from the outside, the tow groups were displaced in order from smallest total displacement to the largest. The steps shown in Figure 9 continued until the final tow groups were sheared. For pre-shearing configurations that skipped tow groups, the teeth for the skipped groups were left open, but the same process was followed.

After shearing, the perpendicular lines previously drawn on the fabric were used to measure the actual displacement distance from the original position for each group of tows using a straightedge aligned with the outside non-displaced tow groups and a digital caliper to measure the distance to the edge of the line as shown in Figure 19. This ensured that the profile matched the distance predicted by the draping software. The final preparation of the fabric was to cut off the ends of the fabric so that only the interior 76.2cm (30in) remained. The ends were discarded due to distortions caused by the clamps.

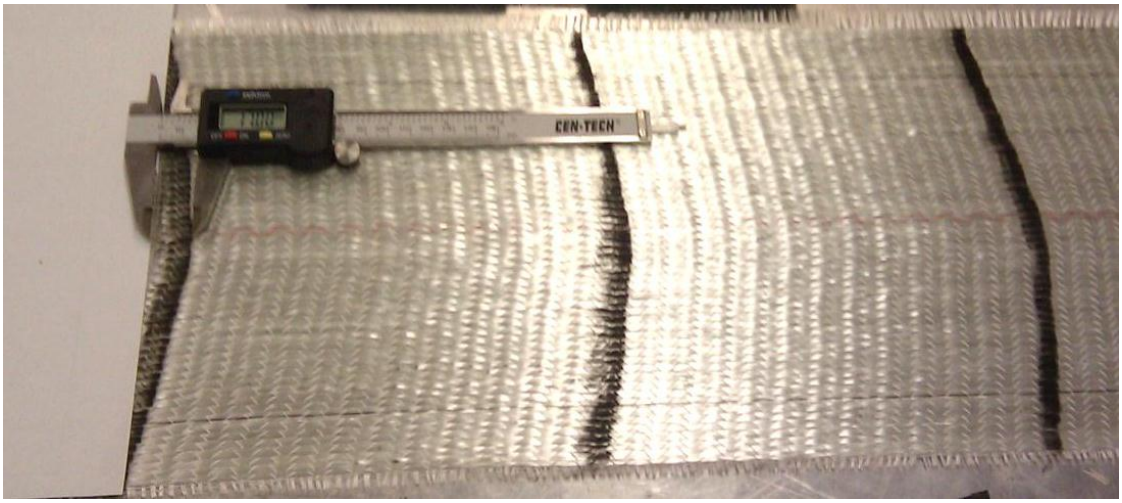

Figure 19. A caliper is used to measure the amount of displacement for the center group of tows. A perpendicular line representing the original position of the tows is made by connecting the outer un-displaced groups with a straight edge.

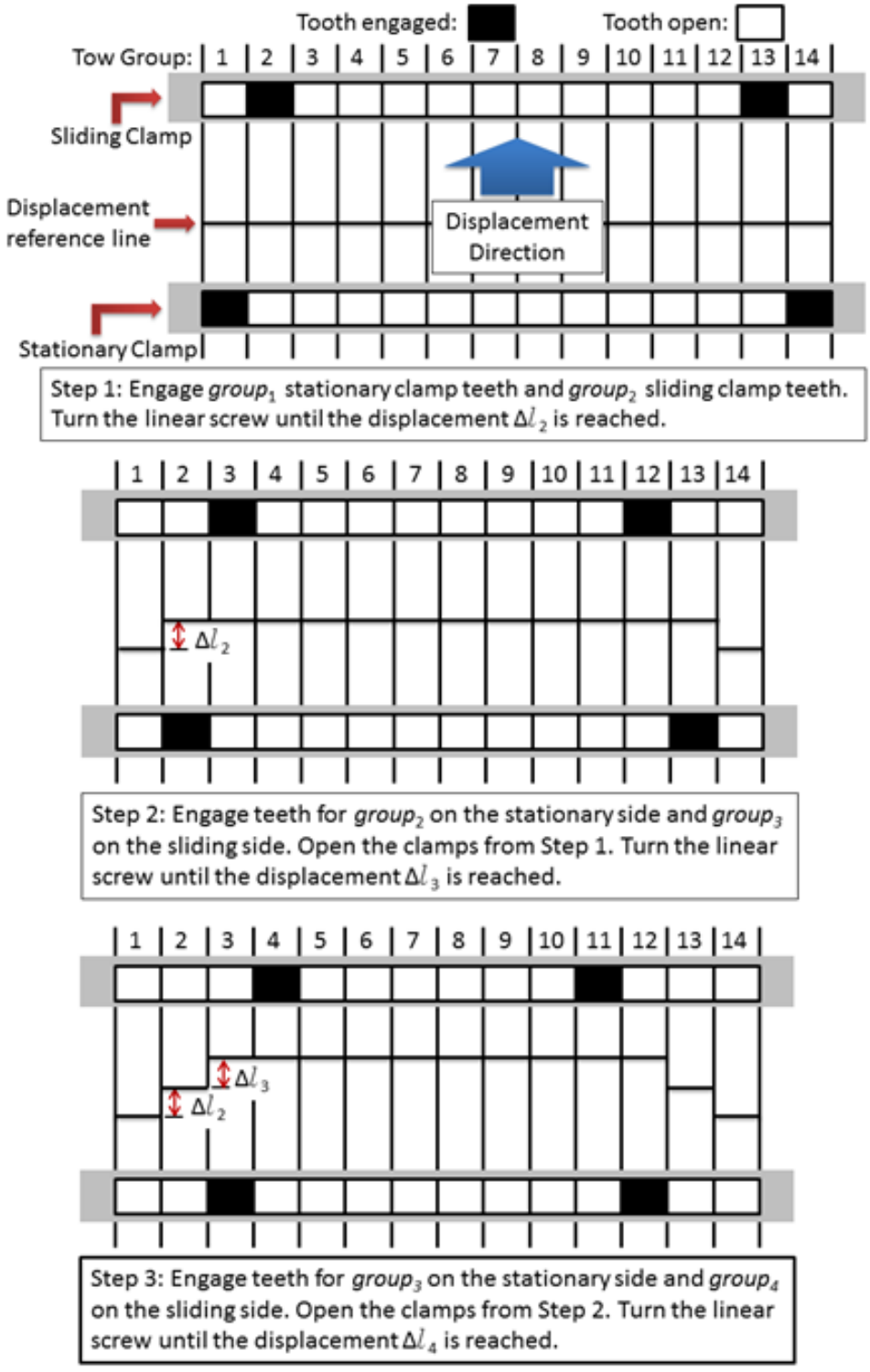

Figure 20. The first three steps of the pre-shearing process for a symmetric profile.

Shearing Misalignment Compensation

Sample sets B and C required some additional compensation during the displacement manipulations on the device. Due to the lateral cinching of tows, which reduces the width of the tow, that is inherent to shearing, the interior tows became misaligned from their teeth on the stationary clamp side after the first displacement was completed as shown in Figure 21. To compensate for this, the teeth were released from both ends and the entire fabric was shifted toward the stationary clamp until the tows were more aligned with the clamp. This compensation was acceptable because it caused no changes to the tow displacement or spacing in the portion of the fabric that would be used for final testing. The alignment was never perfect, so a maximum tow misalignment of one was allowed for these samples. This caused one tow to remain un-sheared with the outermost group and the tow on the inside of the next tooth to be clamped. This was only an issue for the second set of tow groups clamped for both sample set B and C. The remaining tow groups reverted to being well aligned with their respective teeth. This method chosen for realignment was the only option available that provided the desired shear profile while working within the limitations of the shearing device and excluding any forceful manipulation of the fabric by hand.

Figure 21. The tow misalignment after the initial displacement that can be seen in the fourth tow group (*blue lines*). It was caused by the cinching of the interior tow groups. The red arrow shows the second tow group stretched out to compensate.

Fabric Deposition

The samples were then placed into the mold, aligned down the center, and clamped at the seed position as shown in Figure 23. The samples were smoothed into position by hand with a smoothing device (having the complement geometry of the mold cross-section) until the end of the mold was reached. The smoothing device can be seen in Figure 22. The excess fabric at the end of the mold was allowed to naturally drape over the end.

Data Acquisition

The method chosen for measuring the surface of the fabric in the mold was a 3D laser scan that produced a point cloud for each sample. The scanning device was a FARO Edge with a laser scan arm. A laser scan was chosen because it provides an accurate measurement of any out-of-plane deformations without physically contacting the fabric. A contact method could disturb any deformations and would be susceptible to visual inaccuracies when the deformations are small and difficult to see. The empty mold was initially scanned to provide a consistent nominal surface for comparison. The mold surface point cloud was scanned and meshed in RapidForm XOV2 64 (RapidForm). Three planar surfaces on the mold were chosen to create an alignment datum reference frame so that each point cloud would be in the same coordinate system. The mesh was saved as a .STL file.

Figure 22. The pre-sheared fiberglass ply is placed into the mold and clamped at the seed position.

The nominal mold surface was imported to RapidForm XOV as a "nominal surface" and the mold datum planes were re-measured with the touch ball probe to align the coordinate systems of the nominal mesh and laser scan. The touch ball probe was used because it provided a very accurate datum plane to align with the scan plane whereas re-laser scanning the surface did not provide an alignment. Realignments were performed at several intervals when the alignment was lost. The unique realignments provided slightly different results which were accounted for in all surface displacement analyses. The laser scan of the fabric covered the entire fabric surface. After scanning, the points in the cloud that were outside of the fabric edges were trimmed, limiting the scan region to the fabric only. The 3cm of the fabric near the seed position was also removed because reflections in the area created noisy data. In all samples, this region contained no deformations so eliminating it from analysis did not influence the results. The point clouds obtained from each sample scan were meshed in order to reduce the size of the files and the computing time for the deviation calculation. The mesh density chosen was

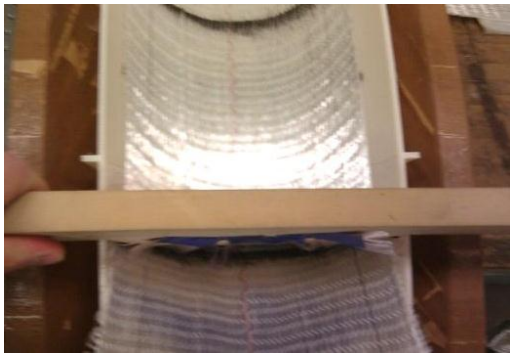

Figure 23. The smoothing device operated by hand.

a “medium” density as defined in RapidForm and a facet count of 750,000 was used. The side length of each triangular facet was roughly 0.7mm.

Data Analysis

Several methods of analysis were used to quantify the severity of out-of-plane deformations present in the samples. The quantity and severity of the waves was used to compare the ability of each sample to conform to the mold surface.

Average Total Deviation

After the mesh was completed a deviation map was created using the “Whole Deviation” function within RapidForm as shown in Figure 24. This deviation map produced an average deviation for the fabric area. This was calculated as the average distance from the nominal surface to the scanned fabric surface. The average deviation selects a group of scanned surface points near a nominal surface point, averages the scanned points, and finds the distance to that averaged point from the nominal point. This distance is the average deviation from that nominal point. The method for calculating the average deviation uses several user defined parameters. The first parameter is a tolerance zone, which eliminates any scanned points that fall outside of the chosen distance normal to the plane of the nominal point. Next, scanned points are eliminated if they fall outside of a specified angle from the surface normal of the nominal. The remaining scanned points are then projected onto the nominal surface in the direction of the nearest normal of the nominal surface. A sphere of user specified radius is created with the nominal point at its center. All scan points projected onto the nominal surface that fall within this sphere can be accepted. The accepted scanned points are

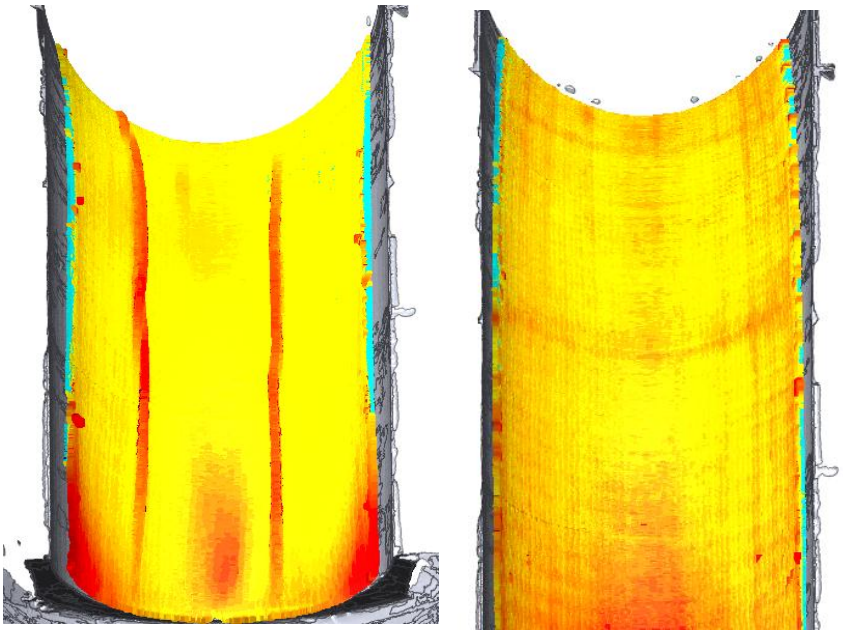

Figure 24. Examples of laser scan point cloud measurements that have been meshed and undergone the "Whole Deviation" function. A sample from group 0 (*left*) produced distinct deformations and a sample from group A (*right*) shows no deformations. The scale of the deviation map is relative to each sample.

averaged and the distance from the nominal to that point is calculated. An example of the point selection and averaging process is shown in Figure 25.

The resulting average deviations were offset by a certain amount stemming from variation in alignments of the nominal surface. To compensate for this, several scans were completed of the empty mold and "Whole Deviation" maps created. The average deviation values from these empty mold scans were subtracted from the average deviations of the fabric scans to compensate for any error between the different alignments. The total average deviation of each sample was used as a measure of overall conformance to compare them.

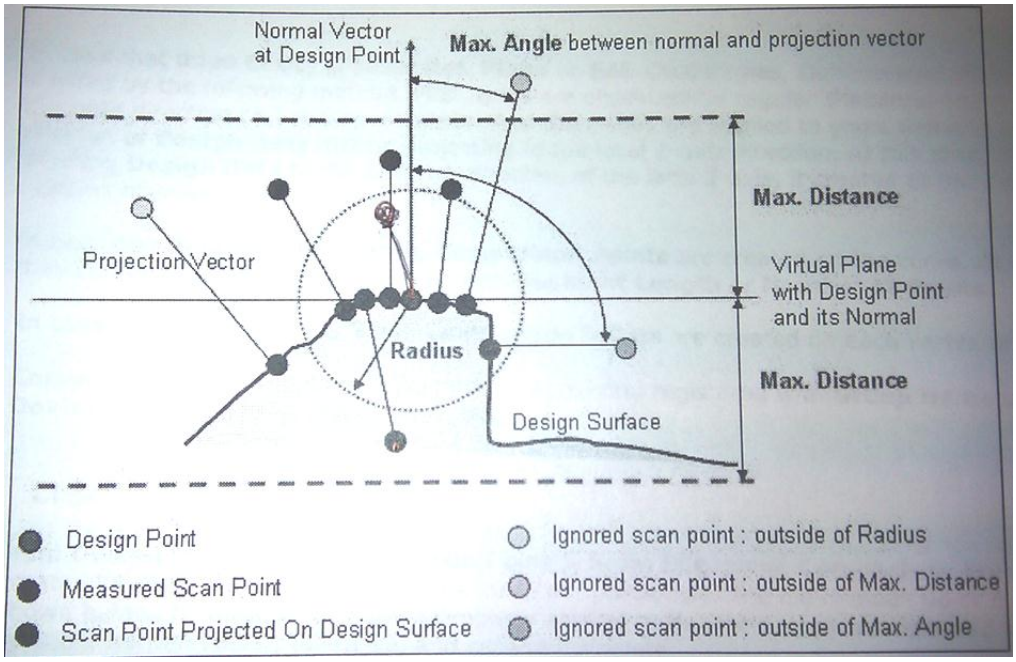

Figure 25. An illustration of RapidForm's "Whole Deviation" function. (RapidForm)

Fabric Thickness Compensation

The comparison of the nominal mold surface scan and the fabric surface scan using the deviation function was essentially a thickness map. When the fabric was in contact with the mold, the resulting scan was a measure of the thickness of the fabric. It is known that when this type of fabric is sheared in the warp direction, it cinches together laterally in the weft direction. This cinching effect was observed to be substantial during the pre-shearing process. As the fiber tows are pushed together, they must deform from flattened oval cross-sections to more circular cross-sections. This results in an increase of the thickness of the fabric. This effect is not inherently detrimental to the mechanical properties of the composite so it was decided to eliminate any difference in thickness from the final

deviation results that were caused by different types of shearing. To accomplish this, a flat plate was initially scanned as the nominal surface. Then each fabric sample, aside from two, were placed onto the plate and scanned. The generated point cloud was then trimmed to the area limited to the fabric and meshed at a "medium level" with 500,000 facets. A "Whole Deviation" analysis was performed. The "Whole Deviation" provided an overall average deviation from the nominal plate surface to the surface of the fabric ply. This overall average surface deviation can be regarded as a measure of the overall average thickness of the fabric. Each sample was scanned while flat to produce an average ply thickness and compared. A statistically significant difference between samples would suggest that pre-shearing caused a substantial change in the fabric thickness which must be accounted for prior to comparing mold conformance. If the difference in average thickness for the flat sample groups was statistically significant then this average thickness would be normalized relative to the lowest average thickness measured. The normalized ply thickness difference would then be subtracted from the average deviation values calculated during the scan of that sample in the mold. If the average thickness difference was not significant it would be regarded as noise in the scans of the fabric in the mold.

Average Deformation Deviation

To isolate significant deviations, all of the fabric surface points were trimmed except for major

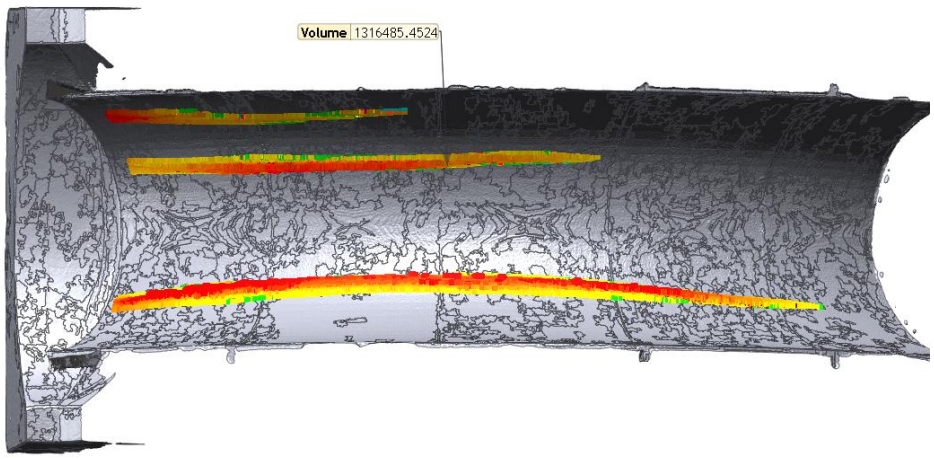

Figure 26. A deviation map limited to the areas of the deformations.

deformations. The acceptable regions were chosen based on the criteria of a rapid change in deviation as it was visualized in the deviation map. Areas of higher than average deviation but no rapidly changing slope were deleted. A "Whole Deviation" was completed for these scans as well,

which provided an average deviation for the deformations only. Figure 26 shows the Whole Deviation map after being limited to the waves only.

Deformation Geometry

Another measure of the out-of-plane deformations was the aspect ratio (AR) of the waves, their length, and frequency. To measure the AR a rotated section view of the total Whole Deviation was created in RapidForm. The views were rotated about the axis of the R1 radius of the mold. The width (L) and height (a) of each wave cross-section was measured as shown in Figure 27 to calculate the AR as shown in Equation 2.

$$AR = \frac{L}{a} \tag{2}$$

The end points of the waves were determined by visually finding the point where the waves transitioned to the surface. The highest point of each wave was used as its height. Each wave was sampled ten times at constant intervals to create an average AR. The lowest AR (i.e., worst case scenario) in any wave was also recorded. The length was simply measured by the central angle of the wave's arc length around the R1 axis.

Deformation Frequency

An additional measure of deformation severity is the number of distinct deformations present in a sample. The frequency of waves in a sample was found by counting the distinctly separate deformations. Separate deviations had to have a transition area between them comprised of a smooth section with distinct and sharp deviation gradient transitions onto each deformation.

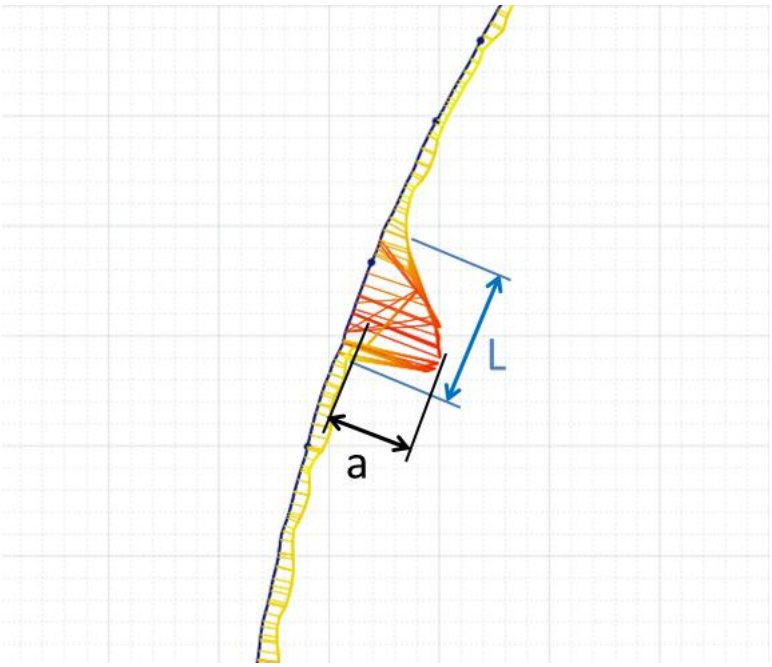

Figure 27. The measurement of AR in a wave cross-section from a RapidForm "Whole Deviation" map.

Chapter 4. Results

Repeatability of Pre-shearing

The first research question asked if it was possible to consistently shear unidirectional non-crimp fabric. Once the relaxation compensation for each group was implemented, the resulting displacements were measured. To compare the samples, the average deviation from the prescribed displacements was calculated for each sample. The average deviation was calculated by averaging the magnitude of the deviation of the tow groups for a sample. The results of the pre-shearing process resulted in a maximum average deviation from the prescribed displacement of 3.2mm in sample GAS4. The average deviation for each sample is given in Table 3. The maximum deviation of an individual tow group was 6.3mm in GAS4. The most difficult tow groups to shear accurately and consistently were those that experienced the highest shear angle and thus the highest amount of fiber compression within a tow. Varying degrees of relaxation from the high shear angle made predictions of what induced displacement would result in the correct permanent displacement. These situations required several attempts at producing the correct profile before a reasonable error was reached. Once the clamps were released the tow compression was relieved and the transverse compression would relax causing a reduction in shear angle as illustrated in Figure 28.

Table 3. Sample average deviation from prescribed displacements.

Sample	Average Deviation (mm)
GAS1	0.6
GAS2	2.6
GAS3	0.7
GAS4	3.2
GBS1	1.1
GBS2	1.0
GBS3	1.7
GBS4	1.5
GCS1	0.8
GCS2	0.9
GCS3	0.7
GCS4	0.5
GDS1	1.3
GDS2	1.8
GDS3	0.7
GDS4	0.4
GES1	0.9
GES2	0.9
GES3	0.5
GES4	0.8

It was also evident that cross-tows were slipping through the stitching in order to maintain the shear profiles as described by the unidirectional inextensible unit cell model. However, this model was not completely supported because cross-tow slipping did not occur until a threshold level of shearing had taken place. The friction between the tows and the stitching had to be broken before slipping could take place. When neighboring tow groups were sheared, as in sample group A, the spacing between the tow groups was defined by the physical clamps. This prevented the outer tow groups from compressing laterally and forced the cross-tows to slip inward through the stitching as they were pulled by the tows being displaced. This was especially evident on the edges of the fabric when the cross-tows were pulled through the outer tow stitching of some samples. Slippage was not the only factor holding the pre-shear profile. Pilot test samples revealed that the shearing was mostly reversible and the samples could return to an initial state. This observation established that friction between the tows caused by lateral compression and friction between the tows and stitching were the major factors holding the fabric together. These findings agreed with those of Bickerton et al. (1997) who found that neither the completely inextensible unit cell nor the unidirectional inextensible unit cell were completely correct. The fabric followed the completely inextensible model until it reached high shear angles where the force on the cross-tows overcame the stitching friction and forced them to slip.

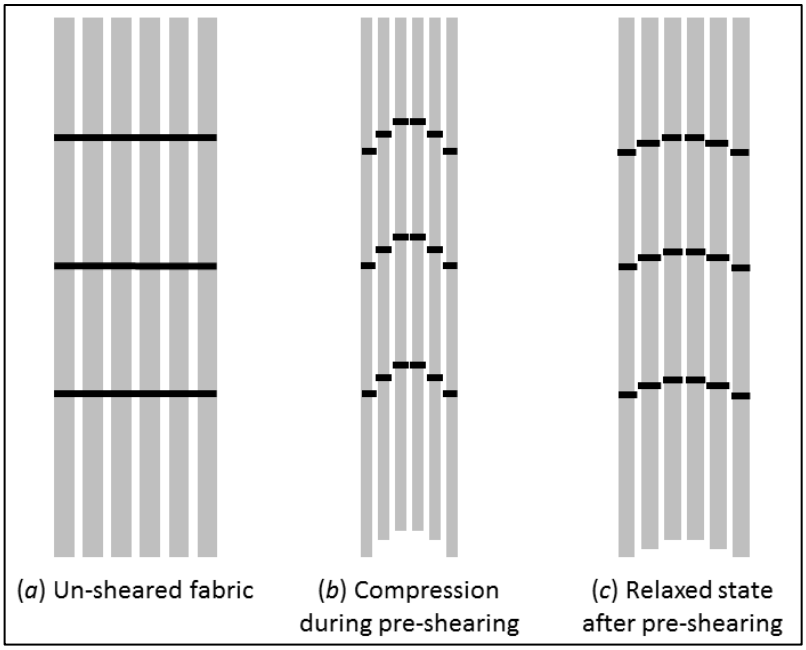

Figure 28. A simplified illustration of transverse compression and relaxation. (*a*) depicts the ply prior to tow displacement. (*b*) depicts the transverse compression that occurs while the fabric is clamped and the tows are displaced. (*c*) depicts the relaxed ply after it has been released from the pre-shearing clamps and the tows have regained some of their width and spacing but have reduced the displacement and shear angle.

Groups D and E were prone to producing out-of-plane deformations while they were being sheared as shown in Figure 29. This was evidence of shear locking taking place during the shearing stage.

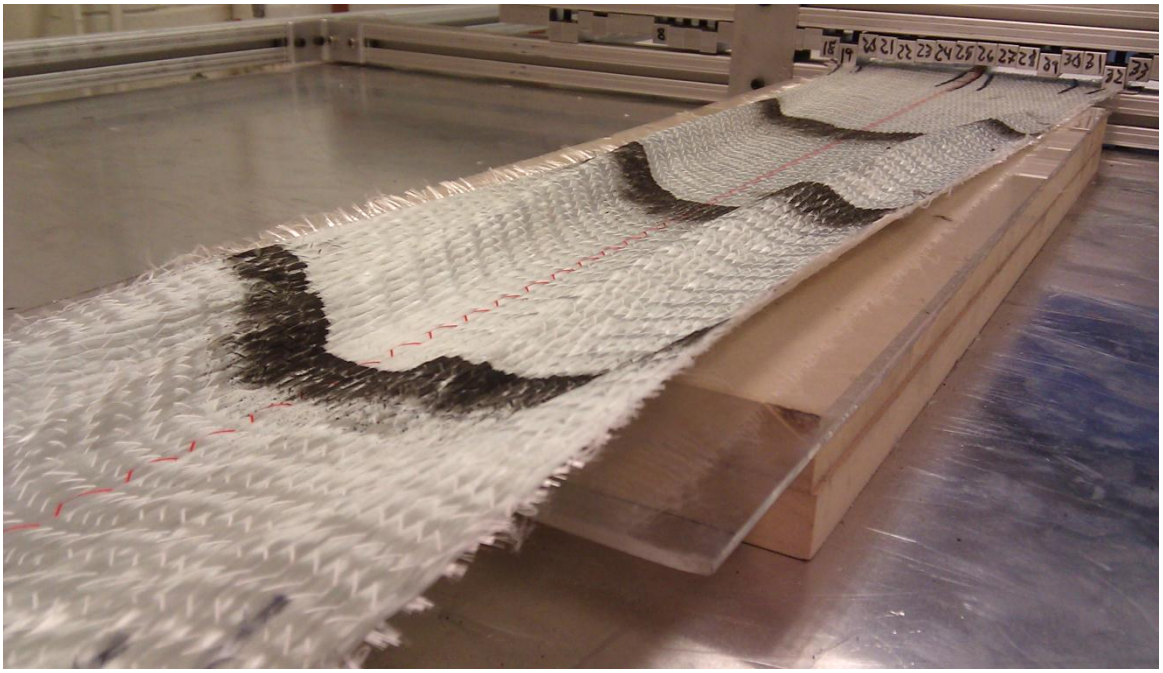

Figure 29. Out-of-plane deformations produced during the shearing of sample sets D and E.

It is likely due to a reduction of the fabric's shear locking limit by the clamping teeth holding the outer sets of tows. The teeth clamping those outer tows prevented the fabric from lateral compression as described in the completely inextensible unit cell model. In this model the warp tows should condense together as they are sheared but the teeth prevented this by constraining the outer tows and cross-tows. The in-plane deformation of the fabric was then effectively limited to the slippage of tows through the stitching. The loss of an outlet for unit cell deformation reduced the shear lock limit of the fabric and caused premature wrinkling. However, the creation of deformations during the shearing process did not result in deformations in the samples, because the deformations were relaxed after the clamps were released and the fabric returned to a flat state.

Feasibility of Low Resolution Pre-Shearing

The purpose of this experiment was to test the ability of a low resolution pre-sheared fabric to conform to a doubly curved mold without producing out-of-plane deformations. The pre-sheared samples (sample groups A-E) were compared to un-sheared control samples (sample group 0) which were all deposited and smoothed onto the mold. Table 4 lists the frequency of deformations of any size in each sample. These deformations were determined from the "Whole Deviation" color maps produced in RapidForm. A deformation was defined as a distinct and rapid color gradient change with higher deviations than the surrounding area. Visual inspection of samples from group 0 showed prominent out-of-plane deformations. These deformations were so severe that the warp tows were forced to double-over themselves creating a wrinkle as shown in Figure 30. All samples from group 0 produced multiple, separate deformations. Three group 0 samples produced three deformations and one produced six. The reason for the large variance of deformations can be linked to the shearing process that occurs during smoothing. Because the un-sheared samples were forced to surpass the shear locking limit over a substantial portion of the end of the fabric, there existed a potential for the deformation to appear in several positions across the width of the fabric. It is likely that during the smoothing process of sample G0S1 the initial deformations formed and allowed the remaining fabric to temporarily relieve its compression. The fabric then formed another deformation in a different downstream location once the shear locking limit had been exceeded. The reason for the deformations occurring in different positions may be due to non-uniformities in the fabric tow spacing and tow width, which may allow for slightly different values of shear locking limit between neighboring tows. In the other three samples where the deformations were more continuous, it may be as a result of the deformation simply continuing along the same tows. In the twenty pre-sheared samples, ten

Table 4. The frequency of defects in each sample.

Sample	# of Defects
G0S1	6
G0S2	3
G0S3	3
G0S4	3
GAS1	0
GAS2	0
GAS3	0
GAS4	3
GBS1	0
GBS2	0
GBS3	0
GBS4	0
GCS1	1
GCS2	0
GCS3	1
GCS4	2
GDS1	0
GDS2	1
GDS3	2
GDS4	0
GES1	1
GES2	1
GES3	1
GES4	3

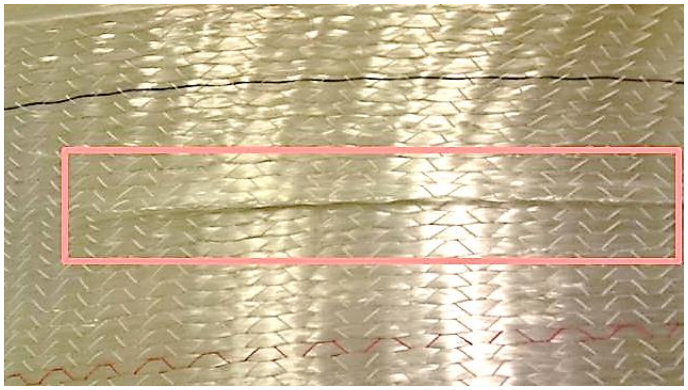

Figure 30. Wrinkle deformation(outlined in red) formed in a group 0 sample.

produced deformations. The majority of those deformations were limited to groups C, D and E. Group A had one sample (GAS4) with deformations and group B had no samples with deformations. The frequency of deformations per pre-sheared sample was also lower than that of the un-sheared samples. The results of the pre-sheared sample tests provide evidence that low resolution deterministic pre-shearing can allow fabric plies to conform to mold geometry under the same conditions where un-sheared plies could not.

The Effect of Tow Grouping Configuration on Out-of-plane Deformations

The out-of-plane deformations in each sample were not all of the same severity. Some deformations were so minute that they were difficult to discern by simple visual observation. To quantify the severity of the deformations, the aspect ratio (AR) was estimated. This AR does not necessarily reflect the same severity of a wave that would appear in the cured part because the effects of resin flow and compression forces introduced by vacuum bagging were not taken into account. Fabric consolidation during vacuum bagging and thermo-mechanical stress during curing and cooling have a large effect on the presence of waves after the part is finished. These factors could reduce or exacerbate the severity of these deformations. However, the AR estimate does provide a means of comparing deformations across all samples. In all samples that produced deformations, the length of the deformation was parallel to the convex curvature. This follows with the expectation that shearing after lateral compression is maximized and the shear locking limit is reached, the fabric will develop an out-of-plane deformation off of the surface that extends along the direction of the tows undergoing compression.

A lower number for AR indicates a more severe slope and thus a more severe wave. The inverse of AR was used so that a larger value would correspond to a larger wave. For the first comparison, each wave was divided into ten equally spaced cross-sections, the AR was measured at each slice, the average of all ten ARs was taken, and the maximum average inverse AR was used to represent that sample. The relationship between defect frequency and maximum average 1/AR as shown in Figure 31 indicates that when more waves are produced, the waves tend to be more severe.

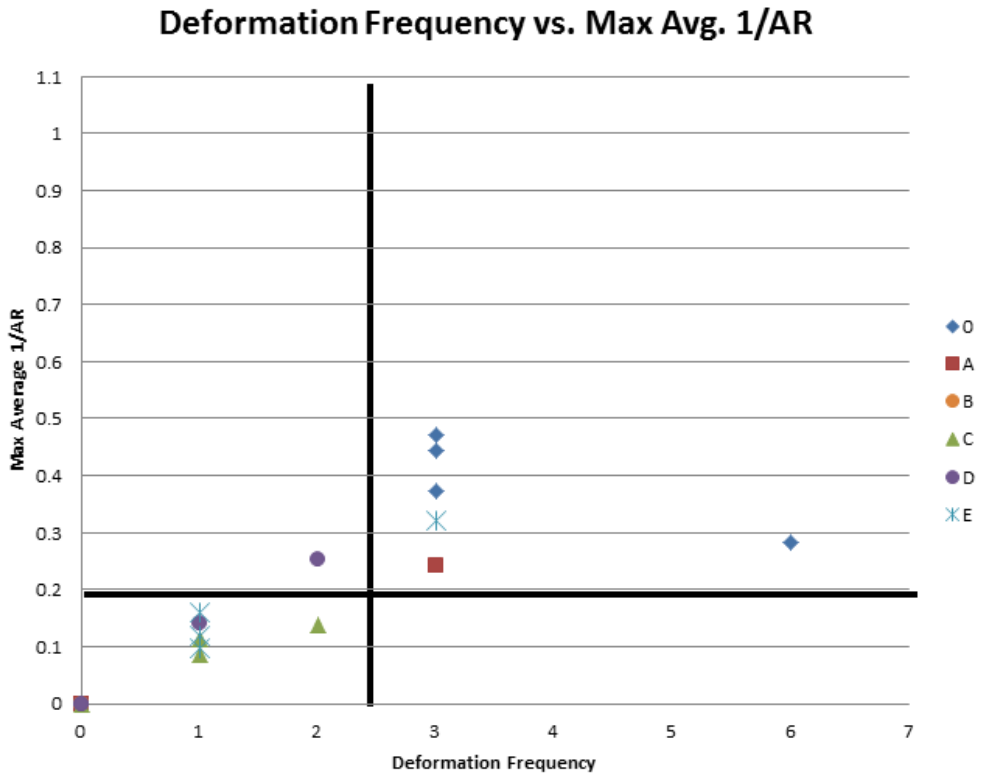

Figure 31. Plot of deformation frequency vs. the maximum average inverse aspect ratio. The darkened lines separate quadrants of low and high frequency and average 1/AR.

A distinct grouping can be seen with AR > 5 (1/AR < 0.2), so 1/AR = 0.2 was designated the threshold between low-severity and high severity AR. For deformation frequency, 2 or fewer was selected as the "low" level. Ten samples had no deformations, which placed them at the (0, 0) point. All four un-sheared samples appeared in the high frequency and high 1/AR area of the graph, which indicated that these samples have the worst conformance. The severity of the deformations in the group "0" samples was actually higher than their position on the plot suggests. At least one of the deformations in each of the samples was in the form of a wrinkle. These types of deformations are automatically deemed defects and much more severe than a wave. This is because a wrinkle causes the tows to acutely bend, which prevents the continuous transfer of load down the length of the tow. A wrinkle can be compared to a cut in the fabric which greatly reduces the mechanical properties and fatigue life. The wave deformations generated in these samples could potentially be acceptable, especially the waves in the low 1/AR quadrant, since they will be compressed during the vacuum bagging stage. If the wave does cause a deformation in the cured sample, it could potentially be at an acceptable AR. The wrinkles are the highest level of severity because vacuum compression will only

increase the severity and there is no acceptable amount of wrinkling. Realistically, the 1/AR for the group "0" samples should be incomparable with the waves due to the extreme severity of a wrinkle. Seventeen of twenty pre-sheared samples appeared in the "Low Frequency" and "Low Avg. 1/AR" indicating that even if they produced deformations they were small.

Another measure of severity was the worst case AR for any cross-section in a sample. The same cross-sections used to determine the average AR of each wave were sorted and the worst AR present on any cross-section was designated to represent its sample. The worst AR did not necessarily occur on the same wave with the highest average AR. The maximum 1/AR was plotted against deformation frequency for Figure 32.

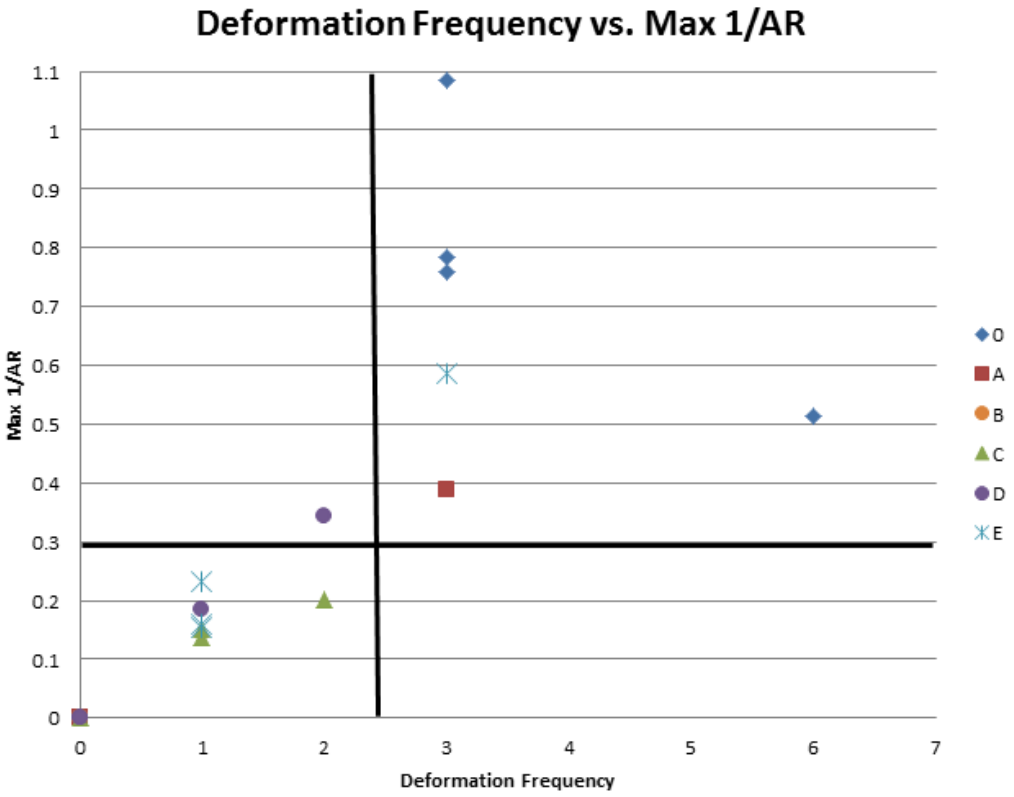

Figure 32. Plot of deformation frequency versus the maximum inverse aspect ratio. The darkened lines separate quadrants of low and high frequency and 1/AR.

The level of the threshold for "Low" maximum 1/AR was raised to 0.3 (AR = 3.3) to accommodate the grouping that was evident. Under these thresholds, this plot follows the same distribution of samples among the quadrants as in Figure 31. When compared with Figure 31, this plot shows that the variance of a wave increases substantially with severity. This can be seen by comparing the max

average 1/AR levels of Figure 31 with those of max 1/AR of Figure 32. The 1/AR in Figure 32 increases drastically as the deformations become more severe. This shows that "High" severity deformations have a high variance of AR compared to the "Low" severity deformations, which have a more consistent AR.

An interesting correlation that is apparent in Figure 31 andFigure 32 is that the severity of waves increases with the frequency of waves. It is evident that when "High" severity out-of-plane deformations are forced to occur, they are numerous. This counters intuitive thinking that would assume that a higher number of deformations would allow the excess material creating them to be distributed over the deformations and result in deformations with lower ARs. This thinking incorrectly assumes that there is a finite length of out-of-plane deformation that must be distributed. This could be attributed to the shearing process that induces deformations in the fabric. Shearing that causes a deformation in one area may induce a deformation in another area, especially as they increase in severity or become a wrinkle. This is supported by the observations of the group "0" samples. During the smoothing process the deformations would form in the predicted area at approximately 60° along the R1 radius and propagate backwards, away from the direction of smoothing. The severe nature of the wrinkles forced the fabric to generate more deformations, even in areas that were previously smooth.

An additional measure of deformation severity is the length of the wave. Because all of the out-of-plane deformations that occurred were concentric with the center of the convex mold curvature along R1, they can be measured in degrees traveled. The longest deformation for each sample was plotted versus deformation frequency in Figure 33. Quadrants were once again selected based on clustering of results. Two deformations were again chosen as the threshold for the frequency axis. The threshold for maximum length was set at 30°. Once again almost all of the pre-sheared samples fall into a group in the "Low Frequency" and "Low Length" quadrant and the un-sheared samples fall into the "High Frequency" and "High Length" quadrant. This provides support for the hypothesis that pre-shearing is an improvement over an un-sheared fabric lay-up.

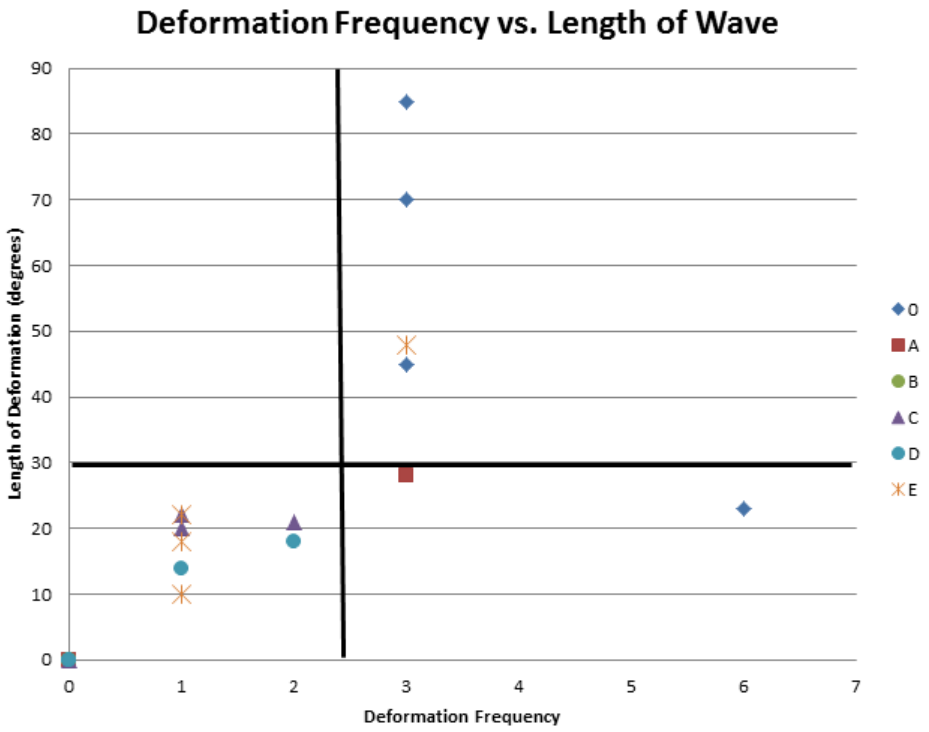

Figure 33. Plot of deformation frequency versus the maximum deformation length. The darkened lines separate quadrants of low to high frequency and length.

The analyses of the fabric surface meshes in RapidForm were intended to result in a measure of overall conformance to the mold. A measure of overall conformance provided a means to directly compare each sample without specific attention paid to the individual deformations. This approach provided a method to compare the conformance of even the smooth samples where deformations were not evident. In this way a more precise comparison of each sample could be made. An ANOVA was performed for the average deviation from the mold surface for the entire fabric surface mesh of each sample group. The differences between the average deviations were within the standard deviations of the groups and therefore not statistically significant. This result indicates that when conformance is averaged over the surface area, deformations are not detected. This may be due to the intrinsically high variance of the fabric. This stems from the periodic nature of the fabric surface distance from the mold surface caused by the tow thickness, which is increased due to lateral compression, and spaces between the tows. This variance hides any deformations which are limited to small portions of the total surface.

Chapter 5. Conclusions

This study provides insights into the effects of pre-shearing fabric on reducing the occurrence of out-of-plane deformations during lay-up. Pre-sheared fabrics can provide substantial benefits for the composites industry. This study also provides an empirical basis for implementing process controls that can produce the correct shear angle distribution in NCF as predicted by computational models from previous research. The broader impacts include a significant increase in component quality and consistency fabricated with NCF, reducing design safety margins, and enabling greater freedom in blade design. Three research questions were posed to determine the feasibility of an automated solution for fabric pre-shearing, namely,

1. Can fabric plies be consistently produced with imbedded shear angle distributions?
2. Will an approximated shear angle distribution reduce out of plane deformations when a ply is smoothed into the mold?
3. What effect does changing the resolution of the shearing profile approximation have on conformance to the mold surface?

An empirical study was conducted to address these questions.

Repeatability of Pre-shearing

To determine the ability of NCFs to retain an imbedded shear angle distribution, shear displacement profiles were generated from a computational model and approximated based on four tow grouping resolutions. Samples were created with a discrete shearing apparatus and the imbedded displacements were measured in three locations. The results of this process showed that permanent pre-shear displacements in NCFs can be consistently produced. It was also observed that fiber slippage of non-crimp fabrics takes place when neighboring tows undergo high levels of shear. Creating plies with an accurate displacement profile must consider relaxation of the fabric. Relaxation was found to be greatest in areas of highest shear, which agrees with pin jointed net models that predicted increased lateral compression forces with high shear angle. The relief of this compression causes a small amount of relaxation. After compensation for relaxation, four samples were created using the same displacements. The maximum error observed for total displacement was 6.3mm error in one case, but over the remaining samples the average accuracy was within 3.2mm. Greater accuracy may be achievable in an industrial process due to the removal of any human interaction, such as turning the linear screw.

The discrete shearing process in some cases caused out-of-plane deformations in the fabric while it was being sheared with the minimum tow configuration resolution. This was attributed to the tow clamps which prevented the lateral consolidation of the warp tows and forced the fabric to relieve the shearing stress by out-of-plane deformation. However, after the clamp constraints were removed, the fabric relaxed and returned to a flat state with the appropriate shear displacement retained. These observations confirm that it is possible to consistently produce discretely pre-sheared plies within an allowable tolerance.

Feasibility of Low Resolution Pre-shearing

To answer this research question, the samples produced on the pre-shearing device were placed into a doubly curved mold, constrained at one end, and then smoothed. Out-of-plane deformations were identified based on the appearance of areas of high deviation gradients. Wrinkle deformations were present in all of the un-sheared samples of the control group and all had multiple deformations. Half of the pre-sheared samples produced deformations of some degree. However, ten samples were produced with no measurable deformations. With the exclusion of only three samples, the pre-sheared groups produced much smaller and less frequent deformations than the control group which produced wrinkle deformations in all samples. The waves were all oriented lengthwise along the convex curve of the mold due to the direction of the lateral compression. The orientation of the deformations would make the small deformations less detrimental to the final part mechanical properties because although the fibers in the waves were not contacting the mold surface, their AR in the warp direction was very high. A low AR deformation in the warp direction would be a greater cause for concern because it creates a more severe disruption along the load path. Since these waves generated lower ARs along the weft direction, the fiber paths in the load bearing warp direction were not highly disrupted. Additional fiber compaction caused during vacuum bagging could completely remove these small defects, making them even less notable compared to the wrinkles of the un-sheared group. This confirms that pre-shearing the fabric into a low resolution deterministic shear angle distribution will allow it to conform without deformations to a mold that is unfeasible for virgin fabrics.

The Effect of Tow Grouping on Out-of-plane Deformations

The samples with the lowest resolution shear displacement profile approximation were found to have more occurrences of waves than high resolution samples. Only a single sample out of the eight highest resolution samples tested produced waves. This provides evidence that higher resolution tow groupings will yield superior conformance results.

Results indicate that the waves produced by all but three of the ten pre-sheared samples with waves were of a relatively low 1/AR. High frequency of deformations were associated with more severe deformations. This result was attributed to high severity deformations inducing additional deformations. Comparing the average 1/AR plot with the worst measured 1/AR plot showed that the variance of the severe waves was much higher than the smaller waves. Neither plot showed evidence that different pre-shearing configurations had an effect on deformation severity when deformations were present. This suggests that the severity of deformations present in the samples in the "Low Severity – Low Frequency" quadrant were at a minimum level of severity for deformations to be measurable.

A plot of deformation length versus deformation frequency showed that the pre-sheared samples had less severe deformations than the un-sheared control group. As in the previous plots, there was no comparable difference among the lengths of deformations for different configurations of pre-shearing. The length of the deformation seems to be independent of the shearing configuration used, but is greatly affected if the deformation is a wrinkle. The wrinkle deformations were observed to be the longest due to their backward propagation after forming.

Additional measurements of overall average deviation showed that there was no statistically significance between samples when wrinkles are averaged over the entire surface. This can be attributed to the relative percentage of the total surface area in which waves occurred.

General Conclusions and Future Work

The purpose of this study was to investigate the process parameters related to pre-shearing NCFs. It has been shown that non-crimp unidirectional fabric can be sheared consistently and that it retains a discretely induced shear angle distribution. Experiments also showed that discrete fabric pre-shearing allowed fabrics to conform to a doubly curved mold that would have otherwise been infeasible. It has also been shown that the resolution chosen for tow grouping configuration has an effect on the presence of out-of-plane deformations and that higher resolutions produce better results. From these observations, it is recommended to use the highest possible resolution that is physically and economically feasible for a particular fabric deposition process. The low resolution configurations are not highly recommended due to the greater potential for deformations and the out-of-plane deformations that occur during the pre-shearing process. It is likely that these deformations will not fully flatten during fabric relaxation.

Extensions to this study could include a longer version of the same type of mold to remove the edge effects observed during lay-up. If the excess fabric at the end of the mold was not left draped over the edge, the presence of waves near the end would be more noticeable and easier to measure. During the pre-shearing process it also became apparent that the location of samples from the fabric roll need to be randomly sampled. Each of the sample groups in this experiment were cut consecutively from the roll. The fabric contains inconsistencies in tow width, tow spacing, and cross-tow edge length, but plies cut near each other will exhibit similar conditions. It would be ideal to cut the samples for each group non-consecutively to distribute the effects of fabric inconsistency.

Additional fabric parameters could be explored to investigate the relationship between tow thicknesses, tow spacing, number of tows, cross-tows, and stitching pattern on the fabric's ability to retain pre-shearing and mold conformability. Additional mold geometry parameters could be explored. Longer, larger diameter molds that are better representations of the large-scale molds used in industry would provide valuable data for the scalability of the process.

Future work towards the development of an automated pre-shearing system can build on the results of this study. A device to continuously imprint fabrics with pre-shearing patterns through the use of rollers could allow fabrics to be unrolled into the device, pass through it to produce the shearing distribution, and then be rolled up again on the other side. In this device, shearing would not be controlled by sliding clamps but through thin differential speed rollers. This process could provide workers with kitted rolls that are unique to specific geometries. The rolls would be supplied to operators as normal and maintain the same production process. Rolls are unrolled onto the molds and smoothed into place by operators with the only difference being that the final shear angle distribution has been predetermined. A further advancement of that solution would be a similar roller device with dynamically variable control that could be programed to imprint a continuously changing pre-shear pattern onto fabric as it is deposited onto a mold. This device could be used to deterministically optimize the shear angle pattern at any location on the mold. This process would minimize the required manual manipulation, which would be limited to accepting the fabric from the device, positioning the fabric, and lightly smoothing it onto the mold. With these advances, the process times can be significantly reduced because the fabric is already smooth. The major benefit would be more accurate and consistent lay-ups which will reduce defects, increase reliability, and allow for lower safety margins.

References

Bickerton, Simon, Pavel Šimáček, Sarah E. Guglielmi, Suresh G. Advani. “Investigation of draping and its effects on the mold filling process during manufacturing of a compound curved composite part.” *Composites Part A: Applied Science and Manufacturing*. 28. 9–10 (1997): 801-816.

Buckingham, R., and G. Newell. "Automating the Manufacture of Composite Broadgoods." *Composites Part A: Applied Science and Manufacturing.* 27.3 (1996): 191-200. Print.

Debout, Pierre, Helene Chanal, and Emmanuel Duc. "Tool Path Smoothing of a Redundant Machine: Application to Automated Fiber Placement." *Computer-Aided Design.* 43 (2011): 122-32.

Dong, L., C. Lekakou, M.G. Bader. “Solid-mechanics finite element simulations of the draping of fabrics: a sensitivity analysis.” *Composites Part A: Applied Science and Manufacturing.* 31 (2000) 639-652.

Hancock, S., and K. Potter. "The Use of Kinematic Drape Modelling to Inform the Hand Lay-up of Complex Composite Components Using Woven Reinforcements." *Composites Part A: Applied Science and Manufacturing*. 37.3 (2006): 413-22. Print.

Hancock, S.G., K.D. Potter. “Inverse drape modelling—an investigation of the set of shapes that can be formed from continuous aligned woven fibre reinforcements.” *Composites Part A: Applied Science and Manufacturing.* 36.7, (2005): 947-953.

Kordi, Tarsha M., M. Husing, and B. Corves. "Development of a Multifunctional Robot End-Effector System for Automated Manufacture of Textile Preforms." Proc. of 2007 IEEE/ASME International Conference on Advanced Intelligent Mechatronics, AIM, Switzerland, Zurich. Piscataway, NJ: Institute of Electrical and Electronics Engineers. 2007. Print.

Lai, Chyi-Iang and Wen-Bin Young. “Modeling Fiber Slippage During the Preforming Process.” Polymer Composites. 20.4 (1999): 594-603.

Lin, H., J. Wang, A.C. Long, M.J. Clifford, and P. Harrison. “Predictive modelling for optimization of textile composite forming.” Composites Science and Technology. 67 (2007): 3242-3252.

Ed. Long, A. C. *Design and Manufacture of Textile Composites*. Cambridge: Woodhead, 2005.

Lukaszewicz, Dirk H.-J.A., Carwyn Ward, Kevin D. Potter. "The engineering aspects of automated prepreg layup: History, present and future." *Composites Part B: Engineering*. 43 (2012): 997-1009.

Magnussen, C. "A fabric deformation methodology for the automation of fiber reinforced polymer composite manufacturing." Thesis. Iowa State University, 2011. Ames: ProQuest/UMI, 2011. Print.

McBride, T.M., Julie Chen. "Unit-cell geometry in plain-weave fabrics during shear deformations." *Composites Science and Technology*. 57.3 (1997): Pages 345-351.

Meng, Fanqi . "Measurement, analysis and process planning for the layup of unidirectional fabrics." Diss. Iowa State University, 2012. Working paper.

Mohammed, U., C. Lekakou, and M. Bader. "Experimental Studies and Analysis of the Draping of Woven Fabrics." *Composites Part A: Applied Science and Manufacturing*. 31.12 (2000): 1409-1420. Print.

Mohammed, U., C. Lekakou, L. Dong, and M.G. Bader. "Shear deformation and micromechanics of woven fabrics." *Composites Part A: Applied Science and Manufacturing*. 31.4 (2000): 299-308.

Potluri, P., and J. Atkinson. "Automated Manufacture of Composites: Handling, Measurement of Properties and Lay-up Simulations." *Composites Part A: Applied Science and Manufacturing.* 34.6 (2003): 493-501.

Potluri, P., S Sharma, R Ramgulam. "Comprehensive drape modelling for moulding 3D textile preforms." *Composites Part A: Applied Science and Manufacturing*. 32.10 (2001): 1415-1424.

Potter, K. "Beyond the Pin-jointed Net: Maximising the Deformability of Aligned Continuous Fibre Reinforcements." *Composites Part A: Applied Science and Manufacturing*. 33.5 (2002): 677-86. Print.

Potter, K. "The influence of accurate stretch data for reinforcements on the production of complex structural mouldings: Part 1. Deformation of aligned sheets and fabrics." *Composites*. 10 (1979): 161-67.

Prodromou, A., and J. Chen. "On the relationship between shear angle and wrinkling of textile composite preforms." *Composites Part A: Applied Science and Manufacturing*. 28 (1997): 491-503.

RapidForm. Help Menu. RapidForm XOV2 64 SP2 2.2.0.0. INUS Technology. 2011.

Rozant, O., P. Bourban, and J. Manson. "Drapability of Dry Textile Fabrics for Stampable Thermoplastic Preforms." *Composites Part A: Applied Science and Manufacturing.* 31.11 (2000): 1167-177.

Rudd, C.D, M.R Turner, A.C Long, V Middleton. "Tow placement studies for liquid composite moulding." *Composites Part A: Applied Science and Manufacturing*. 30.9 (1999): 1105-1121.

Ruth, D. E. and P. Mulgaonkar. "Robotic Lay-Up of Prepreg Composite Plies." *IEEE*. CH2876-1 (1990): 1296-1300.

Shirinzadeh, B. "Fabrication Process of Open Surfaces by Robotic Fibre Placement." *Robotics and Computer-Integrated Manufacturing*. 20.1 (2004): 17-28. Print.

Tam, Albert S., Timothy G. Gutowski. "The kinematics for forming ideal aligned fibre composites into complex shapes." *Composites Manufacturing*. 1.4 (1990): 219-228.

Tucker III, Charles L. "Forming of Advanced Composites." *Advanced Composites Manufacturing*. Ed. Timothy G. Gutowski. New York: John Wiley and Sons, Inc., 1997. 297-372.

Van West, B.P., R.Byron Pipes, M. Keefe, S.G. Advani. "The draping and consolidation of commingled fabrics." *Composites Manufacturing*. 2.1 (1991): 10-22.

Wang, J., R. Paton, and J. Page. "The draping of woven fabric preforms and prepregs for production of polymer composite components." *Composites Part A: Applied Science and Manufacturing*. 30 (1999): 757-65.

Zhu, B., T. Yu, and X. Tao. "An experimental study of in-plane large shear deformation of woven fabric composite." *Composites Science and Technology*. 67 (2007): 252-61.